The Journal of Experimental Biology 214, 3138-3153

doi:10.1242/jeb.057547

RESEARCH ARTICLE

The spatial and temporal patterns of odors sampled by lobsters and crabs in a turbulent plume

Matthew A. Reidenbach[1,*] and M. A. R. Koehl[2]

[1]Department of Environmental Sciences, University of Virginia, Charlottesville, VA 22904, USA and [2]Department of Integrative Biology, University of California Berkeley, Berkeley, CA 94720-3140, USA

*Author for correspondence: reidenbach@virginia.edu

Accepted 20 June 2011

SUMMARY

Odors are dispersed across aquatic habitats by turbulent water flow as filamentous, intermittent plumes. Many crustaceans sniff (take discrete samples of ambient water and the odors it carries) by flicking their olfactory antennules. We used planar laser-induced fluorescence to investigate how flicking antennules of different morphologies (long antennules of spiny lobsters, *Panulirus argus*; short antennules of blue crabs, *Callinectes sapidus*) sample fluctuating odor signals at different positions in a turbulent odor plume in a flume to determine whether the patterns of concentrations captured can provide information about an animal's position relative to the odor source. Lobster antennules intercept odors during a greater percentage of flicks and encounter higher peak concentrations than do crab antennules, but because crabs flick at higher frequency, the duration of odor-free gaps between encountered odor pulses is similar. For flicking antennules there were longer time gaps between odor encounters as the downstream distance to the odor source decreases, but shorter gaps along the plume centerline than near the edge. In contrast to the case for antennule flicking, almost all odor-free gaps were <500 ms at all positions in the plume if concentration was measured continuously at the same height as the antennules. Variance in concentration is lower and mean concentration is greater near the substratum, where leg chemosensors continuously sample the plume, than in the water where antennules sniff. Concentrations sampled by legs increase as an animal nears an odor source, but decrease for antennules. Both legs and antennules encounter higher concentrations near the centerline than at the edge of the plume.

Key words: lobster, *Panulirus argus*, blue crab, *Callinectes sapidus*, olfaction, antennule, aesthetasc, chemoreception.

INTRODUCTION

Animals often use their sense of smell to locate food, identify mates and predators, and find suitable habitats. Odor molecules are dispersed from their source by turbulent wind or water currents. In both terrestrial and aquatic environments, the instantaneous temporal and spatial distribution of odors is complex, and odor plumes are often composed of filaments of chemicals at high concentrations adjacent to fluid with little or no odor (e.g. Crimaldi et al., 2002b). This odor structure varies in a systematic way with distance from the source and depends on factors such as the scale of turbulence in the wind or water flow, and the topography over which the fluid is moving (reviewed in Moore and Crimaldi, 2004; Koehl, 2006; Riffel et al., 2008; Webster and Weissburg, 2009). The spatial and temporal structure of odor concentrations encountered by animals moving in a plume can offer information about the location of the odor source (e.g. Moore and Crimaldi, 2004; Koehl, 2006; Webster and Weissburg, 2001; Page et al., 2011a; Page et al., 2011b) if the animals are able to sample that concentration structure. However, which aspects of the information in an odor plume are used by animals to locate the source are still largely unknown (Webster and Weissburg, 2009).

The first step in the process of smelling is the interception by an olfactory organ of odors in the surrounding air or water. Turbulent wind or water currents in the environment transport chemical signals from a source to an animal's olfactory organs, where small-scale water motion near the olfactory sensilla brings signal-laden air or water close enough to these chemosensory hairs that odorant molecules can diffuse to their surfaces (reviewed by Koehl, 2006; Koehl, 2011). We refer to these physical processes bringing odorants in the environment to the sensilla as odor 'interception', 'encounter', 'capture' or 'sampling' by the olfactory organ. This physical step of odorant encounter corresponds to the delivery to olfactory sensilla of odorants in olfactometers used in neurobiology experiments. After reaching the surface of a sensillum, odorant molecules must diffuse through the cuticle, through the extracellular space and to receptors on the dendrites of olfactory receptor neurons. The patterns of action potentials that these neurons produce in response to the odorants and further processing of these signals in the brain determine whether the odorants are detected by the animal (reviewed by Hildebrand and Shepherd, 1997; Ache and Young, 2005; Wilson, 2008; Su et al., 2009). In this paper we examined how the process of encountering odors by olfactory organs of different designs can be the first step in filtering olfactory information from the environment, before neural processing occurs.

Continuous measurements of concentrations of various tracers at fixed points in plumes have revealed the intermittent nature of chemical signals in turbulent wind or water currents (e.g. Moore and Atema, 1991; Finelli et al., 1999; Murlis et al., 2000; Justus et al., 2002a). However, such continuous measurements do not necessarily represent the temporal pattern of odors arriving at the olfactory sensillae of animals that sniff (i.e. take discrete samples of their fluid environment in space and time) (Koehl, 2006; Koehl,

2011; Schoenfeld, 2006) and that move through the habitat. Thus, the goal of our study was to investigate how the dynamics of sniffing interacts with the fluctuating odor signals at different positions in an odor plume to determine the patterns of odor arriving at olfactory sensillae. We used the olfactory antennules of crustaceans sniffing in turbulent water currents to study this issue because their instantaneous contact with dissolved substances can be observed (Koehl, 2011).

Features of an odor plume that affect behavior

Although early models of odor tracking assumed that animals respond to time-averaged concentration gradients in a plume (e.g. Bossert and Wilson, 1963), the rapidity of plume-tracking maneuvers by crustaceans and insects suggests that they are not using time-averaged concentrations to locate an odor source (Vickers, 2006; Webster and Weissburg, 2009). The plume-tracking success of crustaceans (Weissburg and Zimmer-Faust, 1993; Jackson et al., 2007; Page et al., 2011a) and insects (Willis and Baker, 1984; Justus and Cardé, 2002; Vickers, 2006) is lower in homogeneous plumes than in intermittent plumes, although a few species do not need intermittent odor signals to travel upstream (Justus and Cardé, 2002; Cardé and Willis, 2008). Many types of aquatic crustacean (reviewed by Webster and Weissburg, 2009; Page et al., 2011a; Page et al., 2011b) and terrestrial insects (e.g. Vickers and Baker, 1994; Vickers and Baker, 1996; Mafra-Neto and Cardé, 1995; Mafra-Neto and Cardé, 1996) (reviewed by Cardé and Willis, 2008) find the source of an odor plume by casting back and forth transverse to the moving fluid, but move upstream when they contact odor filaments. Therefore, successful plume tracking depends on flow sensors as well as olfactory sensors for both aquatic (e.g. Atema, 1998; Derby et al., 2001; Grasso, 2001; Steullet et al., 2002; Mellon, 2007; Webster and Weissburg, 2009) and terrestrial arthropods (reviewed by Cardé and Willis, 2008).

Studies of arthropods tracking odor plumes have revealed a number of aspects of the distribution of odor concentrations in a plume that correlate with animal behavior. For example, the frequency of encounters with odor filaments affects plume tracking. Pulses of odors stimulate crabs to walk upstream, and their walking speed and the duration of their bouts of upstream movement increase if the frequency of odor encounters is raised (Keller and Weissburg, 2004; Page et al., 2011a). Likewise, the frequency of odor encounters by crayfish affects their walking speed (Wolf et al., 2004). Insects spend more time flying upwind, have straighter trajectories and find the odor source sooner when the frequency of encounters with odor filaments is increased (Mafra-Neto and Cardé, 1995; Mafra-Neto and Cardé, 1996; Mafra-Neto and Cardé, 1998; Willis and Avondet, 2005). If the rate of intercepting odor filaments is $\geq$10 Hz, moths fly upstream continuously (e.g. Mafra-Neto and Cardé, 1995; Justus et al., 2002b; Cardé and Willis, 2008), and it has been suggested that the frequency of encounters with pheromone filaments by male moths indicates their distance from the female (Lo Iacano and Reynolds, 2008; Stengl, 2010). Odor concentrations typically fluctuate more slowly in water than in air (Moore and Crimaldi, 2004), and the frequency of odor pulses that stimulate upstream locomotion is lower for aquatic crustaceans than for terrestrial insects (e.g. Page et al., 2011a).

The duration of an odor pulse (reflecting the width of an odor filament) can affect plume-tracking behavior. For example, moths fly upstream for longer periods when exposed to odor pulses of greater duration (Mafra-Neto and Cardé, 1996) (reviewed by Cardé and Willis, 2008). Similarly, the duration of the odor-free gap between pulses (indicating the spacing between filaments and the degree of meander of the plume) (e.g. Page et al., 2011a) can affect behavior. The success of crabs at finding an odor source decreases when they experience longer gaps between odor pulses (Keller and Weissburg, 2004; Page et al., 2011a). Furthermore, crabs respond more quickly to odor pulses if the time since the last pulse is $\leq$1000 ms (Page et al., 2011a).

Instantaneous concentrations of odor filaments may also affect plume-tracking behavior. Crabs are less successful at finding an odor source if the concentration of the odor pulses they encounter is lowered (Keller and Weissburg, 2004). However, Page and colleagues argue that the only important aspect of odor concentration is whether it is above the threshold to elicit a response by the animal (Page et al., 2011a). Computational modeling shows that the use of both concentration and frequency of odor pulses increases effectiveness in locating an odor source (Lo Iacono and Reynolds, 2008).

Arthropod responses to odor pulses can occur rapidly. For example, crabs begin rapid locomotion only 500–600 ms after their antennules intercept an odor pulse (Page et al., 2011a), and moths start flying upwind ~200 ms after their antennae are hit by an odor pulse (Mafra-Neto and Cardé, 1996; Cardé and Willis, 2008).

Features of odor stimuli that affect neuron firing

There are marked similarities in the neural olfactory pathways in different phyla (reviewed by Hildebrand and Shepherd, 1997; Ache and Young, 2005; Wilson, 2008; Su et al., 2009), and temporal patterns of neuron activity play a role in olfactory coding in many types of animal (reviewed by Laurent et al., 2001; Stengl, 2010; Junek et al., 2010). Thus, the temporal patterns of active sampling (sniffing) of the odor environment by an olfactory organ can influence the brain's response to odors (reviewed by Ache and Young, 2005; Wilson, 2008), and temporal properties of the stimuli used in neurobiological experiments can affect olfactory coding (e.g. Vetter et al., 2006). Therefore, one of the goals of our study was to quantify natural temporal patterns of odor arrival at olfactory sensillae of animals sniffing in turbulent odor plumes to provide a template for the design of more realistic odor delivery in neurobiology experiments.

When an odor pulse is delivered to the aesthetascs on the antennule of a spiny lobster, *Panulirus argus*, or a clawed lobster, *Homarus americanus*, receptor neurons in the antennule respond (after a latency period of ~70–500 ms) with a series of action potentials (spikes) that lasts ~100–200 ms, followed by a period of decline in the frequency and amplitude of spikes (e.g for a 200 ms odor pulse, spike frequency is 50% of maximum after 420–600 ms and firing ceases after 1500 ms) (e.g. Marschall and Ache, 1989; Gomez and Atema, 1996a). The total number of molecules encountered during an odor pulse does not affect receptor neuron firing patterns (Gomez and Atema, 1996a). In contrast, the greater the rate of change in odor concentration (onset slope) and the bigger the amplitude of the increase in concentration, the shorter the latency period to the neuron's first action potential and the sooner the neuron attains its maximum firing rate (Gomez and Atema, 1996a; Marschall and Ache, 1989). Both maximum spike frequency and total number of spikes also correlate with the onset slope and amplitude of concentration change above background (Gomez and Atema, 1996a; Gomez and Atema, 1996b; Zettler and Atema, 1999; Marschall and Ache, 1989; Derby et al., 2001). Therefore, Gomez and Atema suggested that the onset slope of a pulse of odor might provide information about the lobster's distance from an odor source (Gomez and Atema, 1996a). In contrast, the concentration of odor pulses delivered to moth antennae has no effect on electroantennogram recordings (Murlis et al., 2000).

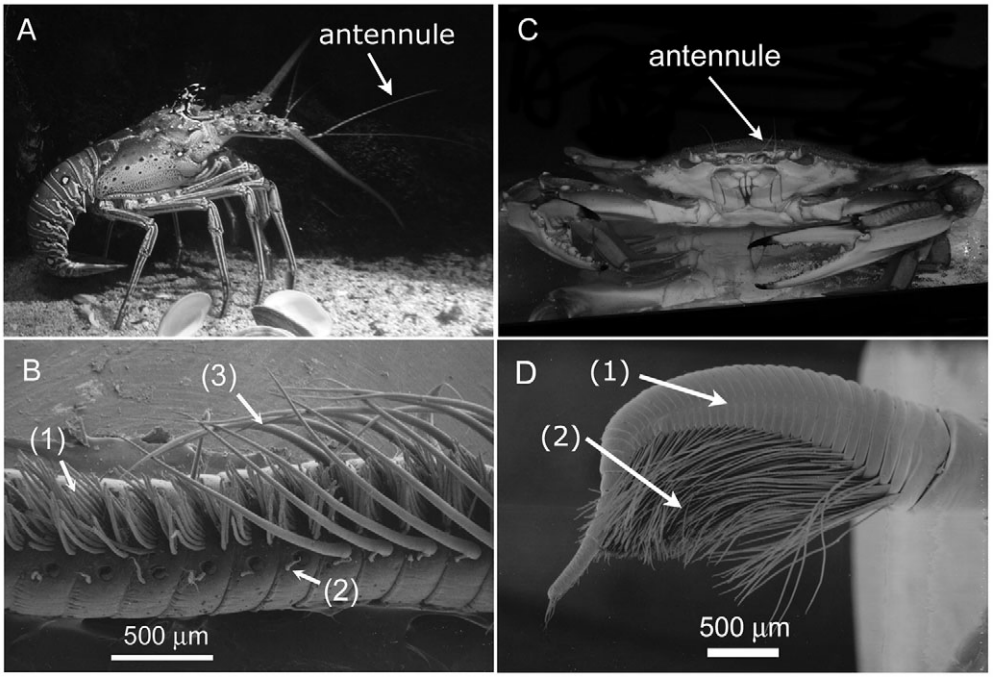

Fig. 1. (A) The spiny lobster, *Panulirus argus*, with the lateral filament of the right antennule labeled. (B) Scanning electron micrograph of a section of the lateral filament of the antennule of *P. argus* showing (1) the chemosensory aesthetascs, (2) the mechanosensory sensilla and (3) the guard hairs. The guard hairs on the left (distal) side of the image have been removed to expose the aesthetascs (photo by J. Goldman). (C) The blue crab, *Callinectes sapidus*, with the left antennule labeled. (D) The antennule of *C. sapidus* showing (1) the lateral filament and (2) the chemosensory aesthetascs (photo by M. Martinez).

Although changes in odor concentration affect receptor neuron firing in *P. argus*, they do not appear to alter neural coding of odor type or behavioral discrimination between different odors (reviewed by Derby et al., 2001).

The duration of a pulse of odor is important in neural coding. For example, the antennal receptor neurons in *H. americanus* require at least 50 ms of odor stimulus to fire, but ≥200 ms for the spike frequency to reflect the concentration increase of the odor pulse (Gomez and Atema, 1996a). For bees, an odor pulse must last 50–150 ms for the coding scheme of projection neurons in the antennal lobe that identifies odorant type to be established (Krofczik et al., 2008). However, if an odor stimulus lasts too long, chemoreceptor cells undergo adaptation (i.e. their response to another odor pulse of the same or lower concentration is reduced or absent). Lobster antennule receptor neurons start to adapt after continuous exposure to an odor stimulus of 300 ms, and are completely adapted after 1000 ms exposure (Gomez and Atema, 1996a). Such adaptation resets the sensitivity of the neuron such that it can respond to pulses of odor concentration higher than background, thereby remaining sensitive to transient increases in odor concentration in environments where the background concentration varies (Borroni and Atema, 1988; Gomez and Atema, 1996b). Lobster olfactory receptor neurons also undergo cumulative adaptation (i.e. repeated odor pulses cause a gradual increase in latency time and decrease in number of spikes), which is more pronounced if the frequency of odor pulse delivery is high (Gomez et al., 1994).

The duration of odor-free gaps between stimulus pulses also affects the responses of olfactory receptor neurons, which recover from adaptation over time. In *P. argus*, disadaptation of olfactory receptor neurons takes several seconds (i.e. the neuron firing in response to a second odor pulse has the same frequency and amplitude as that to the first pulse) (Corroto and Michel, 1998). In *H. americanus* the recovery of receptor neurons (measured by the number of spikes fired in response to an odor pulse) is 20% after an odor-free gap of 1000 ms and 50% after 5000 ms, but total recovery takes 10–30 s (Gomez and Atema, 1996b).

The frequency of repeated odor pulses affects neural responses. If an odor stimulus starts ≥400 ms after the previous one ends, antennule olfactory receptor cells of *H. americanus* can resolve them as separate pulses, but if it arrives ≤200 ms after the previous odor stopped, then the neuron responds as though the second pulse is a continuation of the previous one (Gomez and Atema, 1996b). These neurons show flicker fusion (i.e. respond to successive odor pulses as though they were one continuous pulse) at frequencies of 2–3 Hz (Gomez et al., 1999), but populations of cells can resolve pulses at 2 Hz (Gomez et al., 1994). The bursts of firing by antennule olfactory receptor neurons of *P. argus* adapt selectively to odor pulses at frequencies of 0.5–0.1 Hz (Marschall and Ache, 1989). Moth antennal receptor cells can resolve odor pulses at 2–5 Hz (Rumbo and Kaissling, 1989) but show flicker fusion at 10 Hz (Justus and Cardé, 2002), while electroantennograms show that odor pulses of 5–33 Hz can be resolved, depending on the type of odorant and species of moth (Bau et al., 2002; Bau et al., 2005; Justus et al., 2005; Tripathy et al., 2010). The output of the moth olfactory antennal lobe, where local field potentials can track pulses up to 30 Hz (Tripathy et al., 2010), also varies with the frequency of signal input (Vickers et al., 2001). The intermittency of odor pulses may be enhanced by projection neurons in the antennal lobes, which produce bursts of spikes separated by periods of inhibition (Lei et al., 2009).

Olfactory antennules and sniffing by crustaceans

Antennules are involved in the detection of distant odor sources that motivate upstream locomotion in lobsters [*P. argus* (Steullet et al., 2002; Horner et al., 2004; Garm et al., 2005); *H. americanus* (Devine and Atema, 1982; Atema, 1998)], crabs [*Callinectes sapidus* (Keller et al., 2003; Page et al., 2011a; Dickman et al., 2009; Page et al., 2011a)] and crayfish [*Procambarus clarkii* (Monteclaro et al., 2010)]. The olfactory antennules of decapod crustaceans have two branches (filaments) (Fig. 1). The lateral filament bears rows of chemosensory hairs called ‘aesthetascs’ (reviewed by Ache, 1982; Koehl, 2006) containing the dendrites of chemosensory neurons that

project to the olfactory lobes of the brain (Ache and Derby, 1985; Grunert and Ache, 1988; Horner et al., 2004).

Malacostracan crustaceans flick the lateral filaments of their antennules through the water. During the rapid downstroke of the antennule flick of lobsters and crabs, water flows between the aesthetascs (Mead and Koehl, 2000; Reidenbach et al., 2008; Koehl, 2011), but does not appreciably alter the filamentous structure of odors within the ambient flow (Koehl et al., 2001; Koehl, 2006; Koehl, 2011; Reidenbach et al., 2008). During the slower return stroke and during the stationary pause between flicks, water does not flow through the aesthetasc array (Mead and Koehl, 2000; Reidenbach et al., 2008; Koehl, 2011). Therefore, the sample of water that moves into the aesthetasc array during the downstroke is trapped between the aesthetascs during the return stroke and pause (Koehl et al., 2001; Mead, 2002; Koehl, 2006; Koehl, 2011), which last long enough for the odor molecules in the trapped water to diffuse to the surfaces of the aesthetascs (Stacey et al., 2002; Reidenbach et al., 2008). The next downstroke replaces that water with a new sample; hence, each flick can be considered a 'sniff'.

When an antennule flicks in an odor plume, it only encounters the thin slice of water through which it flicks. It is possible to sample an odor plume on the same fine spatial and temporal scale as an antennule using a technique called planar laser-induced fluorescence (PLIF) (e.g. Crimaldi, 2008; Crimaldi et al., 2002b). A fluorescent dye seeping from a source into flowing water is used as an analog for a dissolved odor. A thin slice of the dye plume is illuminated by a sheet of laser light and recorded by video; the brightness of pixels in each video frame can be calibrated to provide an instantaneous map of 'odor' concentrations in the water. PLIF studies of dye (i.e. odor) concentrations within the aesthetasc arrays of lobster (Koehl et al., 2001) and stomatopod (Mead et al., 2003) antennules flicking in turbulent odor plumes in a flume revealed that the fine filament structure of the plume is not disrupted during the flick downstroke and is retained in the aesthetasc array during the return stroke. Therefore, to determine which aspects of a plume an antennule samples when it sniffs, the odor concentrations in the aesthetasc array at the end of each downstroke must be measured.

There is great diversity in the morphology and flicking kinematics of the lateral filaments of the antennules of malacostracan crustaceans, so they provide good systems for exploring the consequences of antennule structure and motion in terms of how an odor plume is sampled. Although PLIF measurements have been made during plume tracking of odor concentrations intercepted by flicks of stomatopod antennules (Mead et al., 2003) or of concentrations near crab antennules (Jackson et al., 2007; Dickman et al., 2009; Page et al., 2011a), comparison of the temporal patterns of plume sampling by antennules of different design, flicking in the same location in the same plume, has not yet been done. We used two decapods, the spiny lobster, *P. argus* (Latreille 1804), and the blue crab, *C. sapidus* Rathbun 1896, to study how differences in antennule morphology and motion affect the concentration and temporal patterns of odor signals captured at different positions in an odor plume.

Morphology and kinematics of the antennules of *P. argus* and *C. sapidus*

The structure and motion of the long antennules of *P. argus* (Fig. 1A) have been described in detail (Goldman and Koehl, 2001). The lateral filament of the antennule of an adult *P. argus* has a mean length of 60 mm and width of 1 mm. The distal end (~27 mm) of the antennule bears the aesthetascs and guard hairs (Gleeson et al., 1993). The aesthetascs (mean diameter 22 μm) are arranged in rows (10 hairs per row) normal to the long axis of the lateral filament of the antennule, and are oriented at angles that produce a zig-zag pattern at the tips of the aesthetascs (Fig. 1B). *Panulirus argus* typically flick the lateral flagella of their antennules several times in a row at frequencies of 0.4–1.5 Hz (Gleeson et al., 1993; Goldman and Koehl, 2001) and then wait for a few seconds, during which they sometimes reposition the antennule, before executing another series of flicks (Goldman and Koehl, 2001). When odors from food are added to the water, the lobsters flick at higher frequencies (up to 3.5 Hz) (Goldman and Koehl, 2001), using the same flick kinematics as before the addition of the odor. The average peak and mean velocities of the lateral filament of the antennule during a flick downstroke are 0.09 and 0.06 m s^{-1}, respectively, but during the upstroke return mean velocity is only 0.02 m s^{-1} (Goldman and Koehl, 2001). The mean duration of the downstroke is 0.10 s, while the upstroke is more variable in duration, but on average lasts 0.34 s.

The lateral filament of the short antennule of a *C. sapidus* (Fig. 1C) is only 2 mm in length (Fig. 1D) and bears a dense tuft of approximately 650–700 aesthetascs (Gleeson, 1982) on its ventral surface. The aesthetascs are 700–1000 μm in length and 10–12 μm in diameter (Gleeson, 1982). Analysis of high-speed videos of *C. sapidus* antennules shows that they flick the lateral filament at a rate of 3 Hz, and that during the flick downstroke, the aesthetasc tuft sweeps through an arc of 113 deg, moving only a short linear distance (0.40 cm) at a velocity of 0.1 m s^{-1} (M. Martinez, U. Lee, and M.A.R.K., unpublished).

Olfactory sensors on walking legs

Both lobsters and crabs have olfactory sensors on their walking legs that are important in cross-stream motion and odor source location [*P. argus* (Garm et al., 2005); *H. americanus* (Grasso and Basil, 2002); *C. sapidus* (Keller et al., 2003; Jackson et al., 2007; Dickman et al., 2009; Page et al., 2011b)]. Leg sensors are located closer to the substratum than antennules, and therefore are likely to encounter a different odor landscape when navigating in a plume.

Objectives of this study

We used PLIF to compare the odor concentrations sampled by crab and lobster antennules and legs in turbulent odor plumes. The specific questions this study addressed were as follows. (1) How do antennule morphology and flicking kinematics affect the temporal patterns of odor concentrations sampled during flicking in an odor plume? (2) How do odor samples taken by each type of antennule depend on their distance downstream from an odor source, and lateral from the centerline of the plume? (3) How do odor samples taken close to the substratum by legs compare with samples taken by antennules flicking higher above the substratum?

MATERIALS AND METHODS

Laboratory flume and odor source

Experiments were conducted in a laboratory flume that was 25 m long, 0.6 m wide and 0.3 m deep, and had a bottom slope of 0 deg to horizontal (Fig. 2). Unidirectional flow was produced by a variable-drive impeller pump located at the downstream end of the tank. The flume was filled with fresh water to a depth (H) of 0.25 m. Three grids (mesh size 1 cm) at the upstream end of the flume conditioned the turbulence and minimized secondary circulation. The walls of the tank were clear glass and the flume floor was painted black to minimize reflection of laser light.

We used dye to study the dispersal of dissolved odors in turbulent water flow. On the macroscopic scale, dissolved chemicals are stirred and transported by moving water, while on

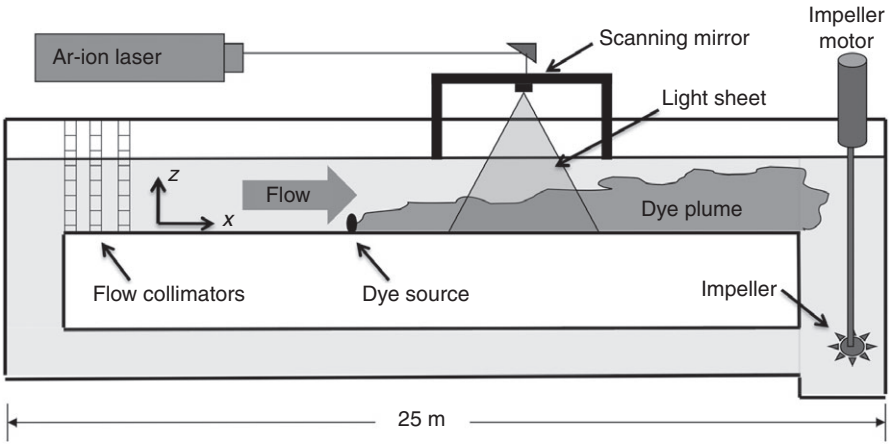

Fig. 2. Schematic diagram of the recirculating flume. The flume was filled to a water depth (H) of 0.25 m. Fluorescein dye was gently injected at the base of the flume through a 1 cm tube at a rate of 0.03 l min^{-1} using a constant-head gravity feed. An argon-ion laser and a moving-magnet scanning mirror were used to create a laser light sheet for visualization of the dye plume.

the microscopic scale mixing occurs by molecular diffusion. The Schmidt number (Sc) represents how quickly momentum structures like eddies in turbulent flow are dissipated by viscosity relative to how quickly chemical structures like odor filaments are dissipated by molecular diffusion:

$$Sc = \nu/D\,, \quad (1)$$

where ν is the kinematic viscosity of water (1×10^{-6} m^2 s^{-1} at 20°C) and D is the molecular diffusivity of the dissolved substance. Most odors that attract lobsters and crabs are composed of amino acids with D of order of 10^{-9} m^2 s^{-1} (Webster and Weissburg, 2009), so we used fluorescein dye (D=5.1×10^{-9} m^2 s^{-1}) as an odor surrogate. This is justified because the Sc number for dye and odors in water is so high (of the order 10^3) that the diffusivity of different molecules has little impact on how they are dispersed in the plume on the scale of millimeters that we measured (e.g. Moore and Crimaldi, 2004; Koehl, 2006). Dye (which we call 'odor' in this paper) was released from a Tygon® tube (1 cm i.d.) through a hole in the base of the flume at a slow rate of 0.03 l min^{-1} from a constant head container that injected minimal momentum into the overlying flow. After each set of experiments at a given velocity, the flume was drained and flushed to remove any residual dye, and refilled before further experiments were conducted.

To ensure that the odor plume was released into a fully developed boundary layer, flow was allowed to develop over a distance of 17 m from the leading edge of the flume before the dye was released into it. Scaling arguments suggest that the thickness (δ) of a turbulent boundary layer grows as fluid moves over a flat plate as:

$$\delta = 0.37L\left(\frac{uL}{\nu}\right)^{-0.2}\,, \quad (2)$$

where u is the mean velocity and L is the downstream distance from the leading edge of the flat plate (Schlichting and Gersten, 2000). For the range of free stream velocities used in our experiments (u=4.6–7 cm s^{-1}), $\delta\geq$0.25 m at L=17 m and further downstream, indicating a fully developed boundary layer throughout the water column.

The position of the odor source parallel to the flow direction was defined as x=0 m, and lateral positions transverse to the flow direction as y=0 m. Water velocity and turbulence were measured using particle image velocimetry (PIV) at a position of x=1.5 m, y=0 m downstream from the source, and dye concentrations were measured at 15 positions downstream from the source, at x=0.5, 1.0, 1.5, 2.0 and 2.5 m downstream, and at each of these distances at y=0, 0.05 and 0.1 m transverse to the centerline of the plume. These locations cover the downstream distance over which lobsters and crabs have been found to be able to reliably orient to odor sources (Horner et al., 2004; Keller and Weissburg, 2004; Weissburg and Zimmer-Faust, 1994). Experiments and boundary layer characteristics are listed in Table 1.

PLIF

Fluorescein dye (i.e. odor) concentrations were measured in vertical planes parallel to the flow direction at different positions in the plume using PLIF. Blue–green laser light (488–514 nm) was emitted by an argon-ion laser (American Laser Corp. 60×, Salt Lake City, UT, USA) at an output intensity of 100 mW. The laser beam was first focused using a 3× laser expander (Melles Griot©, Carlsbad, CA, USA) and then a light sheet was created using a moving-magnet optical scanning mirror (Cambridge Technology model 6800HP; Lexington, MA, USA). The light sheet illuminated a vertical slice through the water column that was 0.2 cm thick and 20 cm wide parallel to the main flow direction. When passed through the laser light sheet, fluorescein dye (peak absorption at 490 nm) emitted light at a mean wavelength of 515 nm (Crimaldi, 2008). Video records of the fluorescing dye within an area of 18×16 cm were made using a 480×420 pixel resolution digital camera (Redlake Motionscope PCI, San Diego, CA, USA) with a 25 mm, f/0.95 fixed lens. The camera was fitted with a 520 nm optical long pass filter (Andover Corp., Salem, NH, USA), which blocked ambient laser light but allowed emitted light from the fluorescing dye to be imaged (Fig. 3). The scanning of the mirror and the camera shutter were synchronized

Table 1. Flow characteristics for the three velocities tested

Experiment	Mean velocity (cm s^{-1})	u_* (cm s^{-1})	z_o (cm)	R^2	Re_*
U1	4.6	0.25	0.005	0.99	6150
U2	5.7	0.31	0.005	0.98	7660
U3	7.0	0.36	0.004	0.99	8900

Mean velocities were measured at 10 cm above the bed. Friction velocity, u_*, and roughness lengthscale, z_o, were computed from a logarithmic fit of the velocity profile using Eqn 2. R^2 is the correlation coefficient for the logarithmic fit. Re_* is the roughness Reynolds number, computed as $Re_*=u_*H/\nu$, where H is water depth in the flume and ν is kinematic viscosity of the fluid.

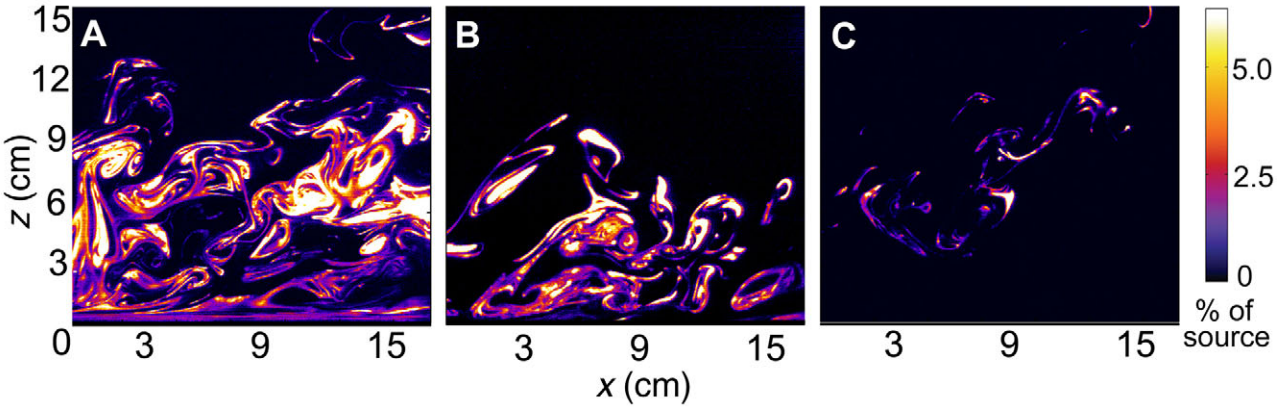

Fig. 3. Instantaneous spatial distribution of 'odor' (i.e. fluorescein dye) concentrations in the water, measured 1.5 m downstream from the odor source at different lateral positions in the plume: (A) along plume centerline, y=0 m; (B) y=0.05 m transverse to the plume centerline; and (C) y=0.1 m transverse to the plume centerline. Color indicates odor concentration, as indicated by the scale bar to the right of the images.

to image the plume at a rate of 60 frames s^{-1}. Therefore, our temporal resolution of concentration changes encountered by a flicking virtual antennule was 16.7 ms. The concentration of the dye source was systematically varied between 20 and 60 µg l^{-1}, with higher source concentrations used when the plume was measured further downstream in order to maximize the full dynamic range of the camera but minimize errors due to photo-bleaching or absorption issues (Crimaldi, 2008). An *in situ* calibration was performed to convert pixel intensity to concentration (for details, see Crimaldi, 2008), and concentrations were normalized as a percentage of source concentration (c_{source}).

Analysis of odor sampled by antennules and legs

PLIF images were used to construct the spatial and temporal variation in odor concentrations sampled along a 'virtual' lateral filament of a *P. argus* antennule and of a *C. sapidus* antennule, each flicking 8 cm above the flume bed. Although both the size of the animal and the positioning of their antennules determines sampling elevation, 8 cm was chosen as a height at which adults of both *P. argus* and *C. sapidus* can actively sample odors. As water only penetrates into the array of aesthetascs of *P. argus* (Koehl et al., 2001; Reidenbach et al., 2008; Koehl, 2011) and *C. sapidus* (Koehl, 2001; Koehl, 2011) during the downstroke of the flick, and because the fine structure of the odor plume entering the aesthetasc array is not disrupted during this downstroke (Koehl et al., 2001; Koehl, 2006; Koehl, 2011), the odor concentrations encountered by a 'virtual antennule' sweeping like a downstroke through an odor plume should be the same as those intercepted by a real antennule during the downstroke (Crimaldi et al., 2002a). The spatial patterns of odor concentrations in the antennule aesthetasc array at the end of the downstroke are retained during the return stroke and the inter-flick pause (Koehl et al., 2001; Koehl, 2006; Koehl, 2011), so we assumed that the concentrations along a virtual antennule in the last PLIF image of a downstroke remained constant until the next flick downstroke.

We took 10 PLIF videos, each consisting of 1024 images and lasting 17.05 s (60 Hz), at each position in the plume, and flicked the virtual lobster and crab antennules through these video sequences using the kinematics and flick frequencies measured for each species, starting the first downstroke in the first frame of each video sequence. For the spiny lobster the 'virtual antennule' was a line 27 mm in length (the portion of the lateral filament bearing aesthetascs) that swept through an arc of 7 deg to mimic the kinematics of the downstroke of the lateral antennule of a *P. argus* (Goldman and Koehl, 2001). The duration of the downstroke was 0.10 s, so we were able to analyze six sequential PLIF images captured in our video during the downstroke. For each of these video frames, we used Image J software to measure the brightness of each pixel along the length of the virtual antennule, and converted that brightness to concentration (techniques described in Koehl et al., 2001; Crimaldi et al., 2002a; Crimaldi, 2008). The flick velocity (u_{flick}) was 6 cm s^{-1}, so the midpoint of the virtual antennule moved a total linear distance of 0.6 cm during the downstroke. This is equivalent to an aesthetasc Reynolds number of 1 (Re=$u_{flick}D_{aesth}/\nu$, where D_{aesth} is the diameter of an aesthetasc and ν is the kinematic viscosity of seawater, 1.05×10^{-6} m^2 s^{-1}). The lobster 'virtual antennule' flicked at a rate of 2 Hz, so 330 virtual flicks were analyzed for the PLIF images captured at each location in the plume. The 'virtual antennule' for the crab was a line 2 mm in length (the portion of the lateral filament bearing aesthetascs) that swept through an arc of 113 deg to mimic the kinematics of the flick downstroke of an antennule of a *C. sapidus* (M. Martinez, U. Lee and M.A.R.K., unpublished). During the downstroke, the tip of the antennule moved a total linear distance of 0.40 cm in a period of 0.04 s (equivalent to an aesthetasc Re of 1), so we could analyze three sequential PLIF images during the crab downstroke. The crab 'virtual antennule' flicked at a rate of 3 Hz, so 500 flicks were analyzed for the PLIF images captured at each location in the plume.

Dye (odor) concentrations encountered by the 'virtual antennules' of the lobster and crab flicking at the same positions in the dye plume in the same PLIF videos were analyzed to compare how these different types of antennule sampled the same odor plume. We measured a number of aspects of the odor samples intercepted by the virtual antennules: (1) concentration encountered by the midpoint of the antennule as a function of time during the downstroke, when concentration could change, and during the return stroke and interflick pause, when concentration remained constant; (2) mean and peak odor concentration for each flick for the whole aesthetasc array of an antennule; (3) width of odor filaments encountered along the length of the antennule at the end of each downstroke; (4) number of filaments intercepted along the antennule during each flick; and (5) percentage of flicks encountering odor. The minimum odor concentrations that can be detected by a lobster or crab are likely to vary for different odors, depending on their chemical composition (Derby et al., 2001; Grasso and Basil, 2002). Therefore, we varied the threshold concentration to explore the effect of antennule sensitivity on the width and number of filaments encountered per flick, and on the percentage of flicks encountering odor. We also examined how these parameters varied with position in the odor

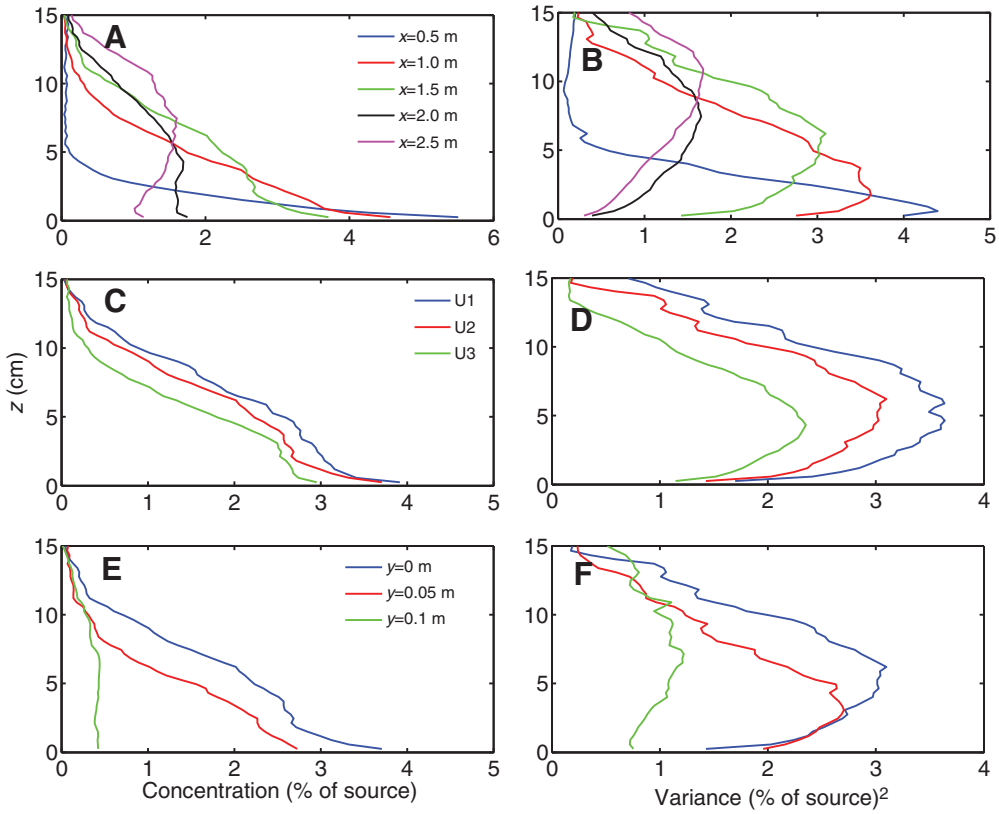

Fig. 4. Vertical profiles of odor concentrations at different positions in the plume. Concentrations are expressed as a percentage of source concentration. For flow condition U2 (Table 1), the (A) mean and (B) variance of odor concentrations at different locations (x) downstream from the plume source along the centerline are shown. For a position 1.5 m downstream from the odor source, (C) mean and (D) variance of concentration along the plume centerline for the three flow conditions measured are shown (Table 1). For a position x=1.5 m downstream from the odor source in flow condition U2, (E) mean and (F) variance of concentration along the centerline, y=0 m, and at positions y=0.05 m and 0.1 m transverse from the centerline are shown.

plume to determine whether they could be used to indicate the location of an animal relative to the odor source.

We sampled the odor plume at a height of 1 cm above the substratum to determine the concentrations encountered by the chemosensors on the legs of lobsters and crabs at the same distances from the source and plume centerline as we measured for the antennules. We compared the mean concentrations encountered by the legs because they do not flick.

RESULTS

Flow profiles

Mean horizontal flow velocities for the three flow regimes and their flow characteristics are listed in Table 1. The friction velocity, u_*, and roughness lengthscale, z_o, were computed by a logarithmic fit to the velocity profile through the bottom 10 cm of the water column using Eqn 3:

$$u(z) = \frac{u_*}{\kappa} \ln\left(\frac{z}{z_o}\right), \quad (3)$$

where $u(z)$ is the mean velocity at a height z above the substratum and κ=0.41 is von Karman's constant (Schlichting and Gersten, 2000). The roughness Reynolds number, Re_*, was computed using Eqn 4:

$$Re_* = \frac{u_* H}{\nu}, \quad (4)$$

where the water depth H=25 cm was used as the characteristic length scale. The drag coefficient, C_d=u_*^2/u^2, due to frictional interaction with the bed of the flume, was computed using, u equal to the mean velocity at 10 cm above the bottom. The C_d was 0.003, which indicates that the bed roughness in our experiments was equivalent to the canonical value typically measured over sands or soft muds (Gross and Nowell, 1983).

Odor plume structure

Average vertical concentration profiles were constructed using 10,000 PLIF images, first by taking the mean concentration at each pixel, $c(x,z)$, and then by averaging horizontally across the imaging area. Examples of such profiles for flow condition U2 (see Table 1) (mean u at 10 cm above the bed was 5.7 cm s^{-1}) are shown in Fig. 4A for positions between x=0.5 and 2.5 m downstream from the source. Even with the extensive averaging (mean of 4.8×10^6 concentration measurements taken for each height), fine-scale spatial variations in concentration were observed as a result of the incomplete statistical convergence of the data. Nonetheless, there was a clear trend of increasing plume height and decreasing odor concentration at greater distances downstream from the source.

A measure of the temporal variability in concentration at a point within the plume is the variance of concentration, σ^2:

$$\sigma^2 = \overline{\left(c - \bar{c}\right)^2}, \quad (5)$$

where c is the instantaneous concentration and $\bar{c}$ is the time-averaged mean concentration (Fig. 4B). The peak variance typically occurred higher in the water column than did the peak mean concentration, indicating that intermittent high concentration filaments occurred away from the bed. In contrast, the reduced variance in odor fluctuations near the bed signifies more complete mixing of the odor plume near the substratum.

To determine how the odor plume structure changed with velocity, profiles of the mean concentration and variance at a position x=1.5 m downstream from the source for the three flow velocities were computed (Fig. 4C,D). Both the mean concentration and variance decreased with increasing mean velocity. Examples of the

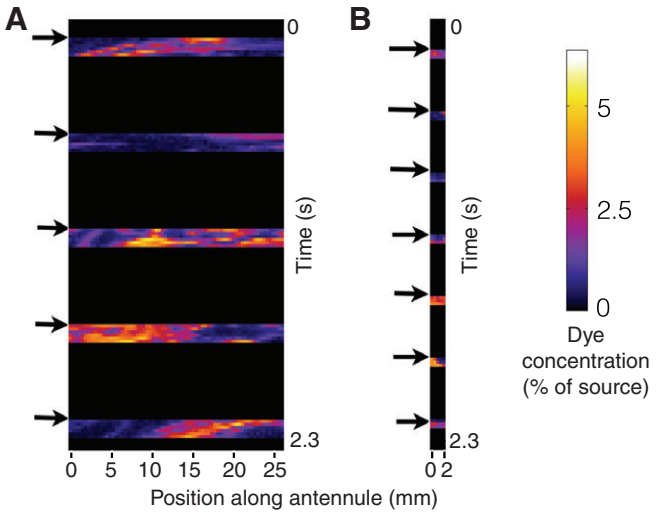

Fig. 5. (A) Concentrations of odor sampled along the length of the lateral filament of a virtual lobster antennule flicking at a rate of 2 flicks s^{-1} at a position 1.5 m downstream from the odor source along the plume centerline. Concentrations are expressed as a percentage of source concentration (scale bar to right of figure). Arrows indicate the start of five successive flicks, each lasting 100 ms. Real antennules retain the concentration pattern trapped within the aesthetasc array at the end of the flick until the next flick replaces that sample with a new one (Koehl et al., 2001). The time intervals between flicks (400 ms, during which the antennule return stroke and the inter-flick pause occur) are shown as black areas so that the different samples taken by each successive flick can be seen more clearly. (B) Concentrations sampled along the length of a virtual crab antennule, flicking at a rate of 3 flicks s^{-1}. Each flick lasted 60 ms, and the duration of the pause and return stroke between flicks is 270 ms.

odor concentration profiles at the plume centerline (y=0) and a different distances laterally from the centerline (y=0.05 and 0.1 m) located at x=1.5 m downstream from the source are plotted in Fig. 4E. The mean odor concentration decreased with distance from the centerline, as predicted for a Gaussian distribution in the transverse direction (Crimaldi et al., 2002b). The variance in odor concentration at these locations also decreased with transverse distance from the plume centerline (Fig. 4F).

Concentration of odor sampled along an antennule

Examples of odor concentrations encountered by the long aesthetasc-bearing section of the antennule of a spiny lobster during the downstrokes of successive flicks are shown in Fig. 5A, and similar concentration maps for the short antennule of a blue crab are shown in Fig. 5B. These maps illustrate the spatial heterogeneity of odors encountered along the length of the antennules, and the variability in odor signal between successive flicks for both the lobster and the crab. The long lobster antennule often intercepts more than one odor filament, whereas the small crab antennule either encounters one odor filament or flicks through odor-free water. These maps were used to determine the temporal and spatial structure of odors sampled at different locations within a plume.

Temporal patterns of odor concentrations sampled

Odor concentrations sampled at different locations in a turbulent plume are plotted as a function of time in Fig. 6. These time series illustrate the intermittent nature of odor encounters by flicking antennules of lobsters (Fig. 6A–C) and crabs (Fig. 6D). Odors are intercepted less frequently at the edge of a plume than at the centerline, where concentration peaks are higher (Fig. 6A *vs* B). The frequency of interception of odor pulses along the plume centerline decreases, while peak concentrations increase as an animal nears the odor source (Fig. 6A *vs* C). The temporal patterns of odor encountered by flicking lobster and crab antennules at a given position in the plume are very similar (Fig. 6C *vs* D), but the periods between pulses of odor tend to be longer for flicking antennules than for a continuous sample of odor concentration at the same position in the plume (Fig. 6C,D *vs* 6E).

Because odor samples are retained in the aesthetasc array during the recovery stroke and inter-flick pause for 290 ms (crab flicking at 3 Hz) to 400 ms (lobster flicking at 2 Hz), we assumed that any odor captured at the end of the flick downstroke represents an odor pulse longer than the 200 ms required for concentration to be reflected by neuron firing (Gomez and Atema, 1996a). Therefore, to summarize the patterns of intermittency of odor samples captured by flicking antennules, we focused on the durations (t_{gap}) of the periods between odor pulses when concentration was below the threshold of 0.25% of source. We separated these odor-free periods into three functional categories:

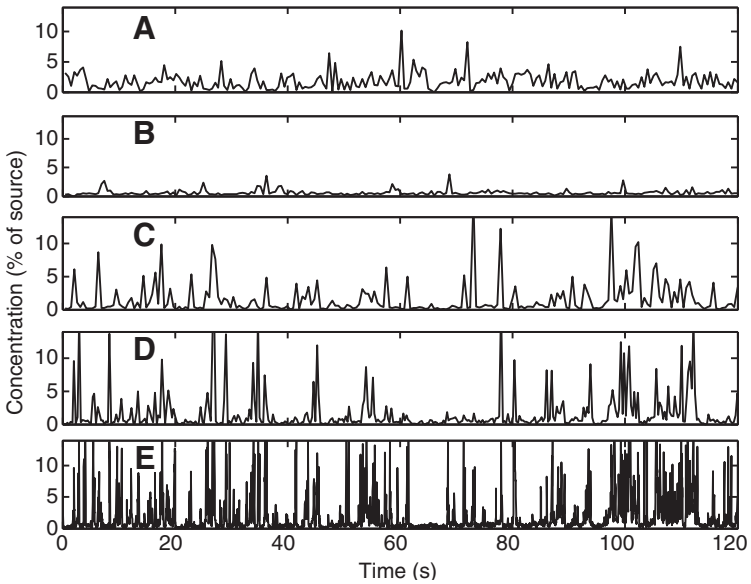

Fig. 6. Odor concentrations encountered at the mid-point along the flicking lobster antennule, plotted as a function of time, for flow condition U2 at (A) x=2.0 m downstream from the source along the centerline (y=0) of the plume and (B) x=2.0 m at a transverse distance of y=0.1 m from the centerline of the plume. Odor concentrations sampled at x=1.0 m downstream from the source along the centerline for the (C) lobster and (D) crab, and (E) when sampling continuously at a rate of 60 Hz.

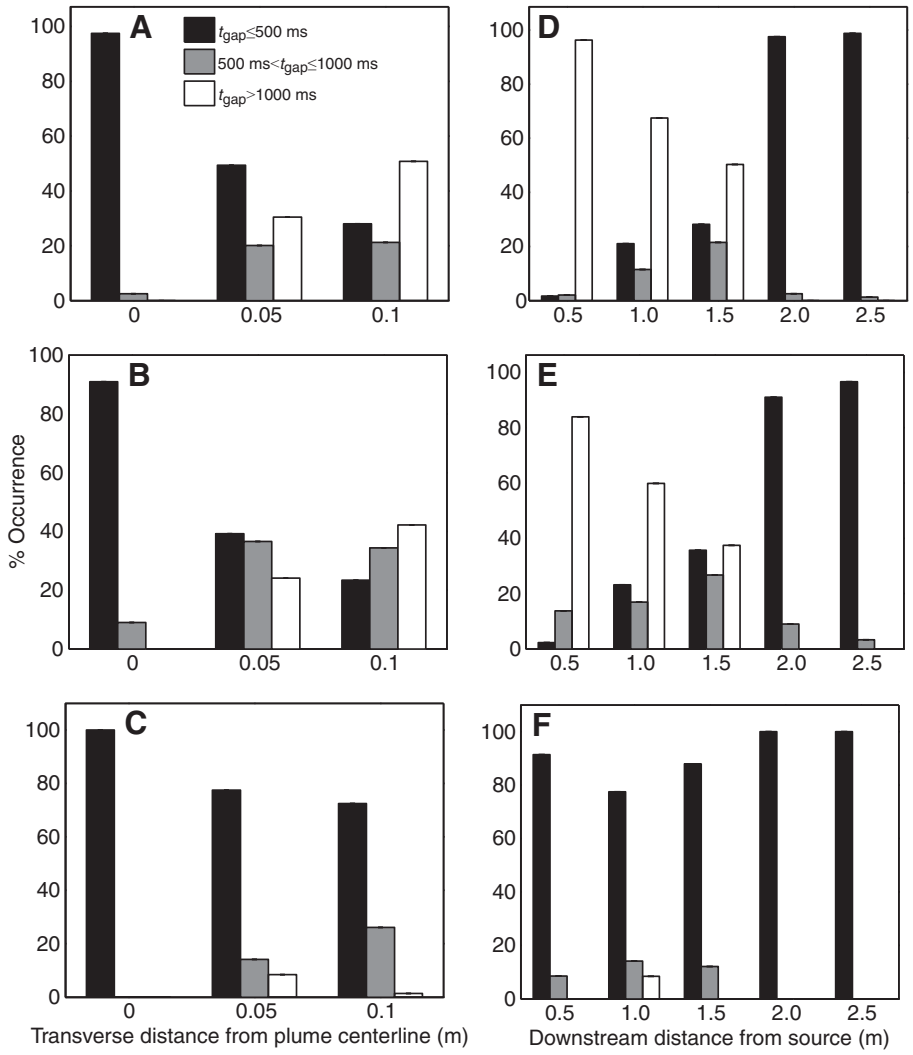

Fig. 7. Percentage of occurrences for which the time gap (t_{gap}) between encounters with odor pulses of concentration c≥0.25% of source concentration c_{source} was ≤500 ms, between 500 and 1000 ms or ≥1000 ms for lobster (A,D) and crab (B,E) flicking virtual antennules, and for continuous sampling at 60 Hz at the same height as the antennules (C,F). These examples were for flow condition U2 at 2.0 m downstream from the odor source at different transverse distances (y) from the plume centerline (A–C), or along the plume centerline at different distances downstream from the source (D–F).

(1) t_{gap}≤500 ms, which corresponds to both lobster and crab antennules intercepting odor during successive flicks, and which is so brief that flicker fusion is likely to occur (Gomez et al., 1994; Gomez et al., 1999); (2) 500 ms<t_{gap}≤1000 ms, when neurobiological (Gomez and Atema, 1996a; Gomez et al., 1999) and behavioral (Page et al., 2011a) data indicate that odor pulses are perceived as separate; and (3) t_{gap} ≥1000 ms, when adapted neurons have recovered ≥20% (Gomez and Atema, 1994) and neurons can synchronize to the frequency of odor pulses [e.g. 0.5–0.1 Hz for *P. argus* (Marschall and Ache, 1989)].

The percentage of odor-free periods in each of these time categories is plotted in Fig. 7 as a function of position in the plume. Most of the gaps between odor pulses sampled by flicking lobster and crab antennules were <500 ms along the plume centerline when the animals were 2.0 m downstream from the odor source, but as the animals approached the source, the percentage of gaps that were of longer duration increased. At a given distance downstream from the source, the percentage of long gaps was greater near the edge of the plume than along the centerline. In contrast to these spatial patterns in odor intermittency shown by flicking antennules, continuous sampling of the odor plume yielded very high percentages of short (<500 ms) odor-free gaps at all positions that we measured in the plume.

Odor concentrations sampled by flicking antennules

The spatial patterns of concentrations sampled by flicking antennules of lobsters and crabs are summarized in Fig. 8. We calculated the mean of the concentrations sampled along the length of an antennule during each flick, and then calculated the mean of these mean concentrations for all the flicks that occurred during a 170.5 s period (totaling 10 replicates of 17.05 s PLIF videos) at each position in the plume for lobsters (Fig. 8A) and crabs (Fig. 8C). The large standard deviations reflect the high variability between the concentrations sampled by individual flicks at each position. We also determined the highest concentration sampled along the length of an antennule during each flick, and calculated the mean of these peak concentrations for all the flicks that occurred during a 170.5 s period at each position in the plume. Although the mean of the mean concentrations sampled by the two types of antennule were similar (Fig. 8A *vs* C), the peak concentrations intercepted by the long lobster antennule were higher than those sampled by the short crab antennule (Fig. 8B *vs* D).

Fig. 9A–D shows the mean of the odor concentrations sampled along a flicking lobster antennule plotted as a function of time for different positions in a plume, while histograms of the number of flicks that encountered odor pulses of different concentrations are shown in Fig. 9E–H. A binomial distribution model (Hays, 1994)

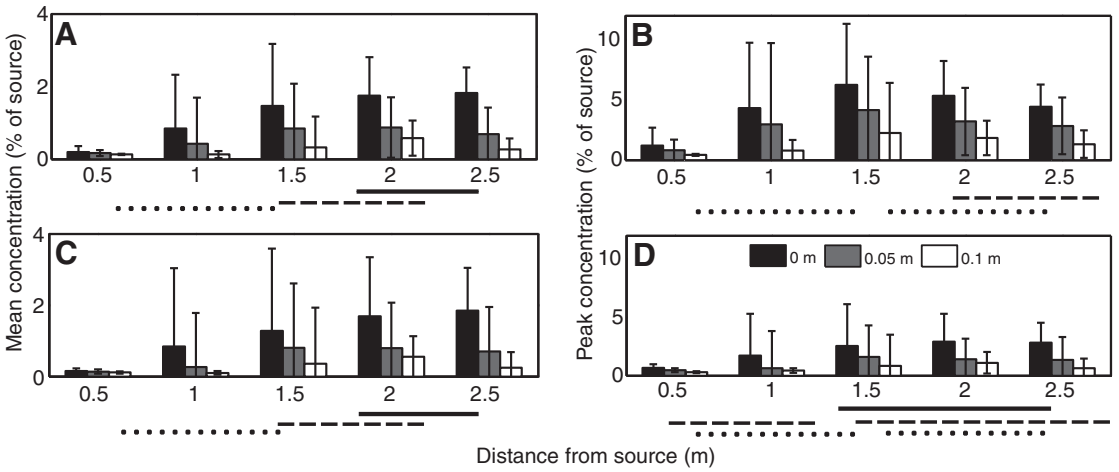

Fig. 8. Odor concentrations intercepted by flicking antennules at different positions in a plume for flow conditon U2. Means for all flicks by a lobster antennule during a 170.5 s period of (A) the mean of the odor concentrations encountered along the length of an antennule during one flick, and (B) the peak odor concentration encountered during one flick. Means for all flicks by a crab antennule during the same 170.5 s period of (C) the mean of the concentrations encountered during a flick and (D) peak concentration encountered per flick. Downstream distance (x) from the source is plotted on the horizontal axis, and transverse distance (y) from the centerline is indicated by the color of each bar. At each position in the plume, the mean of the mean concentrations intercepted by the lobster and crab antennules were not significantly different from each other (ANOVA, $P \geq 0.05$), whereas the peak concentrations were significantly higher for the lobster antennule at each location (ANOVA, $P < 0.05$). Lines under the x-axis connect positions downstream from the source that are not signficiantly different from each other (ANOVA, $P \geq 0.05$) along the plume centerline (solid lines), y=0.05 m transverse from the centerline (dashed lines), and y=0.1 m transverse from the centerline (dotted lines). Error bars show 1 s.d.

was applied to the observed data to test whether the concentration encountered along the centerline of the plume was greater than that encountered at transverse distances (either y=0.05 or 0.1 m) from the centerline. The model assumed that only two outcomes were possible in each of N trials (i.e. concentration at y=0 m is either greater or less than the concentration at y=0.05 or 0.1 m), where each trial is a flick. The probability of success (i.e. detecting odor) for each trial is constant, and trials are independent of each other. Probabilities (P) of encountering higher concentrations along the centerline of the plume than at lateral positions in the plume are plotted as a function of downstream distance (Fig. 10). Both lobster and crab antennules are more likely to encounter lower odor concentrations when flicking at lateral positions in the plume than when flicking along the centerline of the plume. The long lobster antennule sampled a greater area of the plume than did the short crab antennule, and thus the lobster had a greater probability than the crab of sampling higher concentrations along the centerline than at lateral positions in the plume. For both the lobster and crab, the probability of sampling higher concentrations along the centerline *vs* lateral positions decreased as they approached the source.

Both lobster and crab antennules flicking along the centerline of the odor plume had a greater probability of intercepting lower odor

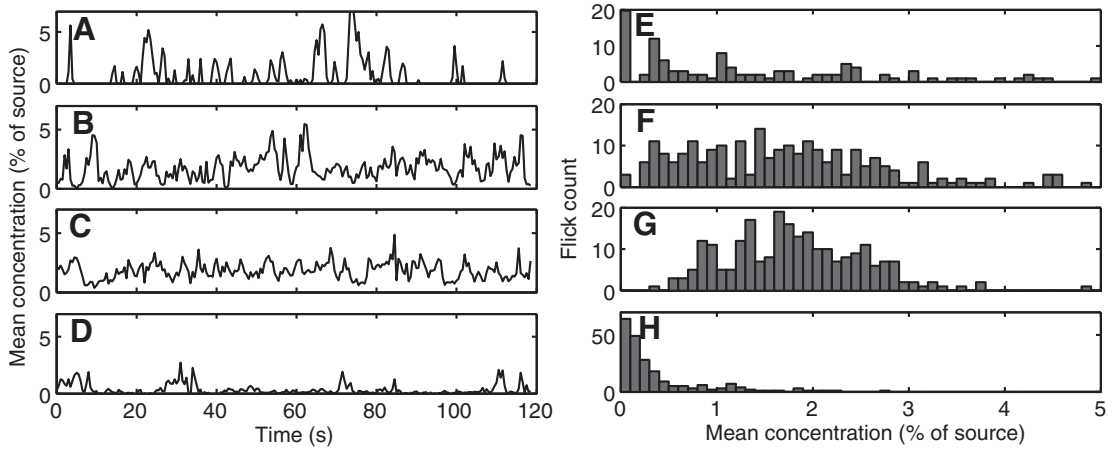

Fig. 9. Mean of the odor concentrations encountered along the virtual antennule of a lobster during each flick, plotted as a function of time for flow condition U2 when the antennule was located at different positions in the plume: (A) x=1.0 m downstream from the source along the centerline (y=0) of the plume; (B) x=2.0 m along the centerline; (C) x=2.5 m along the centerline; and (D) x=2.5 m at a transverse distance of y=0.05 m from the centerline of the plume. During each of the records of 120 s shown, 240 flicks occurred. Histograms of the mean concentrations encountered during a flick: (E) x=1.0 m downstream from the source along the centerline (y=0) of the plume (skewness=13.3); (F) x=2.0 m downstream of the source along the centerline (skewness=0.9); (G) x=2.5 m downstream from the source along the centerline (skewness=0.5);and (H) x=2.5 m downstream from the source at a transverse distance of y=0.05 m from the centerline of the plume (skewness=2.0).

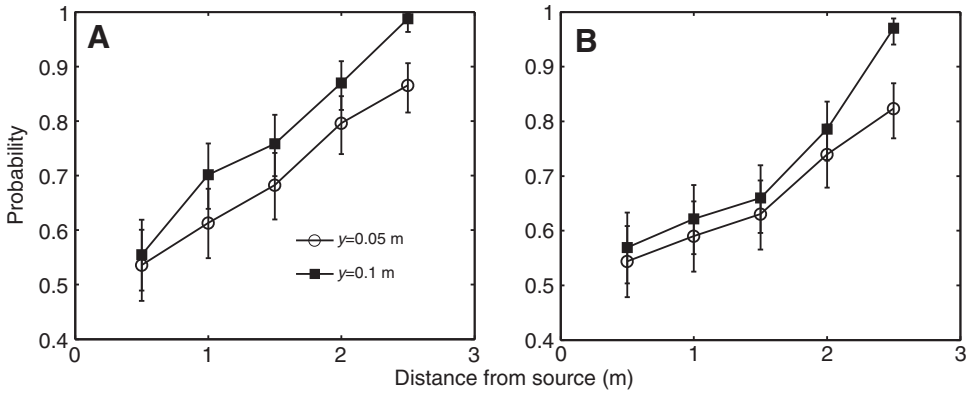

Fig. 10. Probability that an individual flick of (A) a lobster antennule and (B) a crab antennule will sample a greater mean concentration along the centerline (y=0 m) of the plume than at a transverse distance of y=0.05 m or y=0.1 m from the centerline. Error bars show 95% confidence intervals.

concentrations when they flicked near to the source than when they flicked farther downstream (Fig. 11). For example, for the plume generated in flow condition U2, probability P=0.95±0.03 (95% confidence interval) that the mean concentration encountered by an individual lobster flick at x=0.5 m was lower than at x=1.0 m. The lower concentrations encountered near the plume source were primarily due to boundary layer hydrodynamics and the vertical growth of the plume. Antennules flicking at a height of 8 cm above the substratum very close to the source sampled the upper edge of the plume and had fewer encounters with odor filaments than they did further downstream. In contrast, the probability that a lobster antennule encountered a lower odor concentration at a distance of 2.0 m downstream from the source than when 2.5 m downstream from the source was only 0.55±0.06, suggesting that once the plume has reached the height of the antennules, statistical changes in mean odor concentration occur slowly with downstream distance.

Width of odor filaments sampled along an antennule

How each virtual antennule flick sampled the spatial structure of concentrations within an odor plume was examined by measuring the widths of the odor filaments intercepted along the length of an antennule. The widths of odor filaments encountered by lobster antennules flicking at different distances downstream from the odor source along the plume centerline are plotted in Fig. 12A for a low threshold odor concentration (0.25% of source concentration) and a high threshold concentration (2.0% of source). Not surprisingly, the filaments sampled were significantly wider if the threshold concentration was lower (ANOVA, Bonferroni, P<0.05). For a given threshold odor concentration, there was high variability in filament width and there was no statistically significant trend in filament width as the lobster neared the odor source for the low threshold odor concentration (0.25% of source), but a small increase in filament width closer to the source for the high threshold odor concentration (2.0% of source). In contrast, the crab virtual antennule encountered filaments of relatively constant width for a given threshold concentration at all downstream distances tested (Fig. 12B). Because the crab antennule is so small, it can only sample the width of filaments narrower than the antennule length (<2 mm). Therefore, filament width appears to be a poor predictor of location within the plume for both lobsters and crabs.

Number of odor filaments sampled along an antennule

The number of odor filaments intercepted during a flick by a lobster virtual antennule at different distances downstream from the odor source is plotted in Fig. 13A for a low threshold odor concentration (0.25% of source concentration) and a high threshold concentration (2.0% of source concentration). As we wanted to know how many filaments could be intercepted simultaneously by one antennule, we only included in our analysis those flicks that encountered odor above the threshold concentration. The example in Fig. 13 shows the results along the plume centerline for flow condition U2 (Table 1), but similar patterns were measured for the other flow conditions. At low threshold concentration, significantly fewer filaments were intercepted per flick close to the source than farther downstream (Fig. 13A). In contrast, when threshold concentrations were high, fewer filaments were encountered, and there was no statistically significant trend with distance downstream from the source. Crab antennules are so small that when they encountered odor during a flick, they typically intercepted only one odor filament and there was no pattern in the number of filaments captured per flick with distance from the source (Fig. 13B).

Percentage of flicks encountering odor

The percentage of flicks that encounter odor above threshold concentration for antennules of lobsters and crabs depends on their position in the odor plume and on their threshold concentration for odor detection. The examples shown in Fig. 14A and B are for flicks made at various transverse positions (y) relative to the plume midline at a distance of x=2.0 m downstream from the source in flow condition U2 (Table 1), but similar patterns were observed for all

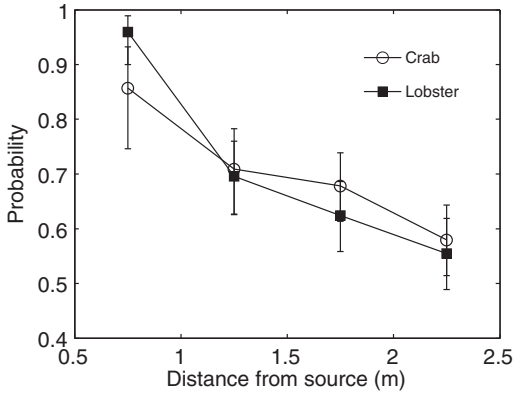

Fig. 11. Probability that a lobster or a crab antennule flicking along the centerline (y=0 m) of the plume at a given downstream distance (x) from the source sampled a greater concentration at that position than it did at a position 0.5 m closer to the source. A probability greater than 0.5 indicates that the flicking antennule, on average, encountered a lower concentration as it moved upstream to a position 0.5 m closer to the source. Values are plotted at the midpoint between the two sampling locations. Error bars show 95% confidence intervals.

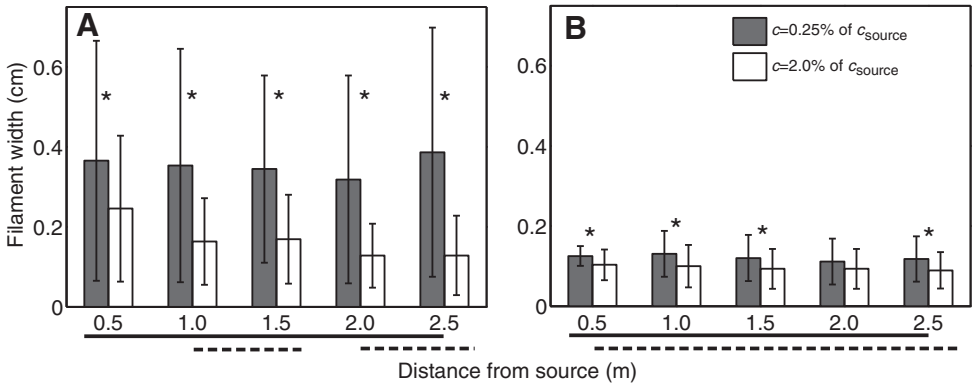

Fig. 12. Mean width of filaments measured along the length of (A) a virtual lobster antennule and (B) a crab antennule, plotted as a function of the distance from the source along the plume centerline for flow condition U2 (Table 1). Grey bars indicate filament width if animals can detect low odor concentrations (threshold concentration, c=0.25% of c_{source}), and white bars indicate filament width for a higher threshold concentration (c=2% of c_{source}). Solid lines below the graphs indicate the positions in the plume at which the number of filaments intercepted per flick is not different for c=0.25% of c_{source}, and dashed lines indicate positions that are not different for c=2.0% of c_{source} (ANOVA, Bonferroni, P≥0.05). Asterisks above the bars at a given position indicate cases where the values for c=0.25% of c_{source} are significantly different from those for c=2.0% of c_{source} (ANOVA, Bonferroni, P<0.05). Error bars show 1 s.d.

flow conditions tested. At a low threshold concentration of 0.25% of source, both the lobster and crab had a greater likelihood of intercepting an odor filament when flicking along the centerline of the plume than when flicking at transverse positions away from the centerline. In contrast, at high threshold concentrations (2% of source), and for the crab antennule in particular, very few flicks encountered odor and transverse position had little effect on the percentage of flicks that encountered odor. For both the lobster and crab antennules at the centerline of the plume at the low threshold (0.25% of source), fewer flicks intercepted odor filaments when the animals were very near to the source than when further downstream, where the plume was taller (Fig. 14C,D). In contrast, for the high threshold concentration (2% of source), the percentage of flicks that intercepted odor filaments varied in a more complex way with distance from the source. Both lobster and crab antennules intercepted fewer odor filaments far (2.5 m) from the source, but experienced higher encounter rates as they moved closer to the source, reaching a maximum encounter rate at a distance of 1.5 m downstream from the source. Then, as both animals approached even closer to the source along the plume centerline, the percentage of flicks encountering odor dropped, as fewer odor filaments reached the elevation of the antennules.

At any position relative to the odor source, small crab antennules were much less likely to encounter odor filaments than were the longer lobster antennules, which sample a larger region of the plume when they flick. Furthermore, the likelihood of sampling odor filaments of high concentration was much lower for the crab antennule than for the lobster antennule.

Odor plume encountered by the legs

Examples of the temporal patterns of odor concentrations encountered by chemosensors on virtual legs of crabs and lobsters at a height of 1 cm above the substratum at different positions in a plume are shown in Fig. 15A–C. Although concentrations at the legs

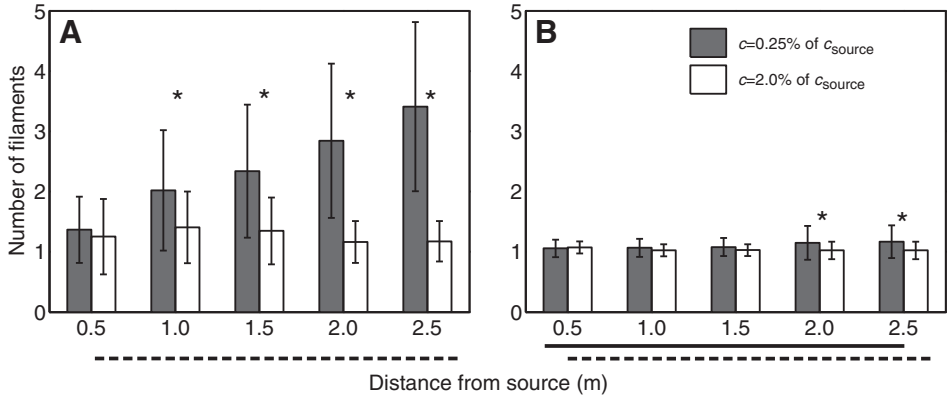

Fig. 13. Mean number of odor filaments intercepted during a single flick along the length of (A) a lobster antennule and (B) a crab antennule, plotted as a function of the distance from the source along the plume centerline for flow condition U2 (Table 1). Grey bars indicate filament width if animals can detect low odor concentrations (threshold concentration, c=0.25% of c_{source}) and white bars indicate filament widths for a higher threshold concentration (c=2.0% of c_{source}). Solid lines below the graphs indicate the positions in the plume at which the number of filaments intercepted per flick is not different for c=0.25% of c_{source}, and dashed lines indicate positions that are not different for c=2.0% of c_{source} (ANOVA, Bonferroni, P≥0.05). Asterisks above the bars at a given position indicate cases where the values for c=0.25% of c_{source} are significantly different from those for c=2.0% of c_{source} (ANOVA, Bonferroni, P<0.05). Error bars show 1 s.d.

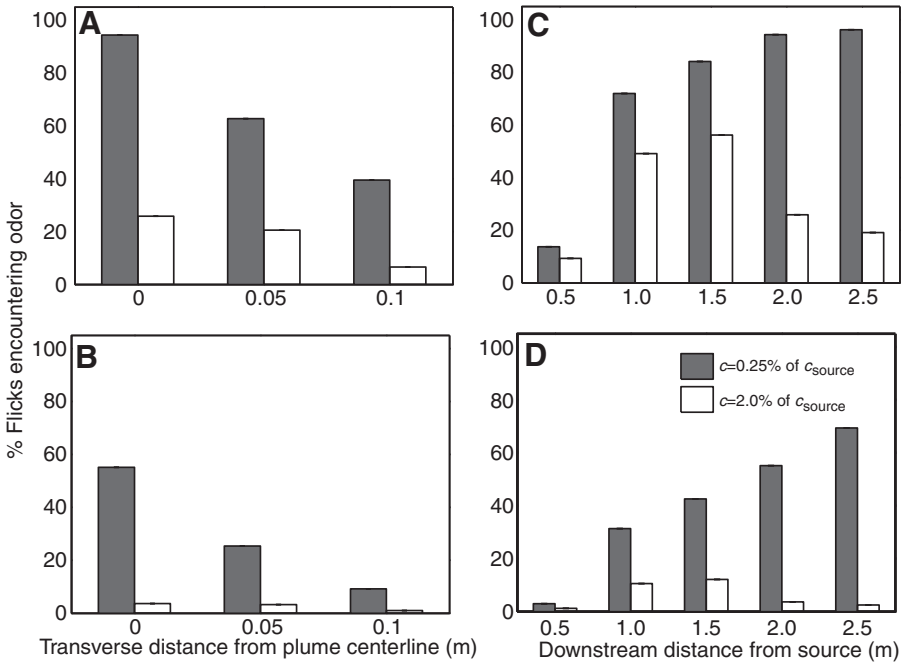

Fig. 14. Percentage of flicks that sampled odor filaments with concentrations greater than or equal to the threshold concentration (c/c_{source}) at different positions in the odor plume for flow condition U2. Grey bars indicate animals that can detect low odor concentrations (c=0.25% of c_{source}) and white bars show animals with a higher threshold (c=2.0% of c_{source}). The percentage of flicks encountering odor for (A) lobster and (B) crab virtual antennules flicking 2.0 m downstream from the source at different transverse distances (y) from the plume centerline, and for (C) lobster and (D) crab virtual antennules flicking along the plume centerline at different downstream distances (x) from the plume source.

fluctuate rapidly with time, the legs experience nearly continuous exposure to odor, whereas flicking antennules at the same distances from the source encounter more and longer odor-free gaps between odor pulses (Fig. 6A–C). Odor concentration sampled by the legs increases as the animals move closer to the source (Fig. 15A *vs* C,D), but the most striking differences in concentration sampled by the legs are between the very high concentrations sampled at the plume centerline and the very low concentrations sampled at the edge of the plume (Fig. 15A *vs* B,D).

DISCUSSION

Odor plumes in turbulent water flow are filamentous and intermittent; thus, odor concentrations sampled by flicking olfactory antennules of benthic crustaceans are highly variable. The features of odor plumes that affect crustacean behavior and neuron firing (reviewed in the Introduction) are the frequency of odor encounters, duration of odor pulses and odor-free periods, and concentration of odor pulses. We found that there are patterns in the odor concentrations sampled by antennules that depend on their morphology, kinematics and location in a plume.

Antennule morphology affects patterns of odor concentrations sampled

Long lobster antennules sample a larger region of a plume during each flick than do short crab antennules. Although the average of the mean concentrations captured during flicks by both types of antennule are similar at each location in a plume, lobsters intercept odors during a greater percentage of their flicks and sample higher peak concentrations than do crabs. However, because crabs flick at a higher frequency than crabs, the durations of odor-free gaps between captured odor pulses is similar for the two types of antennule. While the number and width of odor filaments intercepted during a flick by a lobster antennule varies with position in a plume, a crab antennule is too small to sample such differences. Furthermore, the probability that a lobster antennule samples higher concentrations at the centerline than along the edge of a plume is greater than for a crab. Thus, the spatio-temporal patterns of odor concentrations sampled by animals with different 'nose' designs searching in the same odor plume can be quite different.

Aspects of sampled odor concentration that indicate position in a plume

As odors from a source on the substratum are carried downstream and stirred with the surrounding water, the spatial structure of odor filaments oor in the plume changes (reviewed by Moore and Crimaldi, 2004; Koehl, 2006). For example, a plume increases in height and width with downstream distance from a benthic source. Therefore, as a lobster or crab flicking its antennules at a height of 8 cm above the substratum nears an odor source (<1 m downstream from the source), both the peak and mean odor concentrations of the filaments captured during flicks decrease, and the duration of odor-free gaps between odor pulses increases. During plume-tracking experiments in a flume, PLIF measurements of odors near the antennules of crabs sampled at rates similar to flicking also showed longer odor-free gaps as crabs neared the source (Page et al., 2011a). The surprising decrease in concentration of odors intercepted by antennules when near the source occurs because the antennules only sample the top edge of the plume when they are close to the source. At greater distances from the source, where the plume is taller than the height of the antennules, neither peak nor mean odor concentrations sampled by flicking antennules are good indicators of downstream location relative to the source. PLIF measurement of odor concentrations near the antennules of plume-tracking *C. sapidus* showed that there was no relationship between the concentrations of odor pulses and crab upstream locomotion (Page et al., 2011a).

We found that the concentration of odors encountered by flicking antennules of both lobsters and crabs was greater near the centerline of a plume than at lateral positions closer to the edge of the plume, and odor-free intervals were shorter along the centerline than at the edge. Although these right–left differences are good indicators of lateral position in the plume, the probability of flicking antennules sampling higher concentrations along the centerline than at lateral

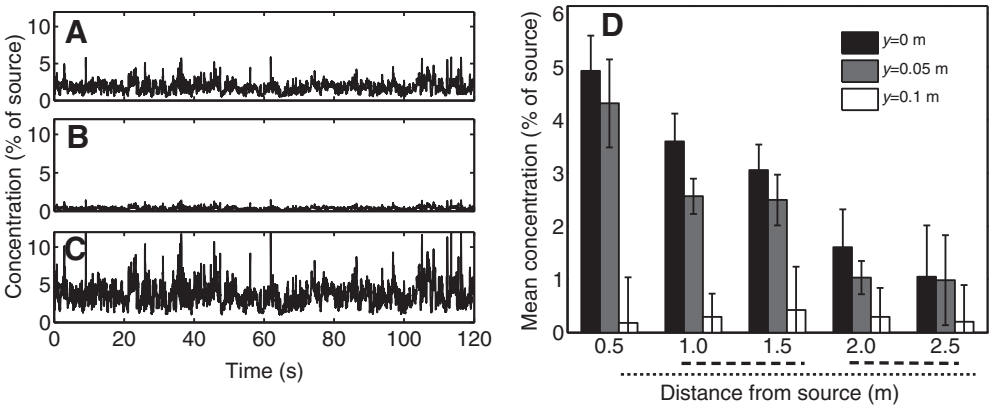

Fig. 15. Odor concentrations encountered in flow condition U2 by virtual walking legs at a height of 1 cm above the bed (location of olfactory sensors on lobster and crab legs), plotted as a function of time at different positions in the plume: (A) x=2.0 m downstream from the source along the centerline (y=0) of the plume; (B) x=2.0 m at a transverse distance of y=0.1 m from the centerline of the plume; and (C) x=1.0 m downstream from the source along the centerline. (D) Mean concentration at 1 cm above the bed as a function of downstream distance (x) from the source, where transverse distance (y) from the plume centerline is indicated by the color of each bar. Error bars show 1 s.d. Dashed lines below the graphs indicate the downstream distances from the odor source at which mean concentrations intercepted at y=0.05 m are not different from each other, and dotted lines indicate positions that are not different at y=0.1 m (ANOVA, P≥0.05). Mean concentrations intercepted at y=0 m are significantly different from each other (ANOVA, P<0.05) at all downstream distances measured. At each downstream distance except 2.5 m, the concentrations at different transverse distances from the centerline are significantly different from each other (ANOVA, P<0.05).

positions decreases as animals near the source, where the plume is both shorter and narrower.

Odor encounter rates by both lobster and crab antennules show a different pattern as animals move through an odor plume. The percentage of flicks that intercept odor filaments increases as animals move upstream towards an odor source, peaking at a distance of 1.5 m from the source, and then declining as animals continue upstream where the plume height becomes ever shorter relative to antennule position above the substratum. In contrast, changes in the percentage of flicks that encounter odor filaments are good predictors of lateral position in a plume for both lobsters and crabs, but only if they can detect low threshold concentration.

A number of features of turbulent odor plumes sampled by flicking antennules are not good indicators of the animal's position in the plume. For example, the widths of odor filaments intercepted by antennules do not vary with location in the plume for both lobsters and crabs. Similarly, for a crab the number of filaments captured per flick is a poor indicator of position in a plume, while for a lobster the number of filaments intercepted per flick only changes with position in the plume if the threshold concentration is low.

Consequences of flicking

Our data comparing continuous samples of odor concentrations at a point with discrete samples taken by a flicking lobster or crab antennule at the same position (Figs 6 and 7) reveal two possible functions of sniffing. (1) Flicking may enhance the ability to distinguish transient increases in odor concentration. When an odor plume is sampled by flicking, the duration of the odor-free gaps between odor pulses is longer than for continuous sampling, thereby giving antennule receptor neurons more time to disadapt before encountering the next odor pulse. This should reduce the chance of flicker fusion (i.e. interpreting two different odor filaments as one) and should counteract the loss of responsiveness to odor pulses in a series due to cumulative adaptation (reviewed in Introduction). The importance of intermittent exposure to odors in enhancing odor detection and offsetting the adaptation of chemosensory neurons has been discussed previously (Ache, 1991; Schmitt and Ache, 1979). (2) Flicking may enhance the spatial information carried in temporal patterns of odor encounters. The temporal intermittency of odor signals sampled by flicking antennules varies with position in an odor plume, but these spatial patterns in intermittency disappear if the same plume structure is sampled continuously (Fig. 7).

There are non-aesthetasc olfactory sensilla on the medial branch of an antennule, which does not flick, and lobsters navigate to an odor source more readily if both antennular chemosensory pathways are operating (Horner et al., 2004; Horner et al., 2007). Whether lobsters use the difference in intermittency of odor encounters by flicking and non-flicking antennule branches at the same height in a plume to help them determine their position relative to the source remains to be studied.

Odor sampling by antennules *vs* legs and plume-tracking behavior

Behavioral studies indicate that the instantaneous spatial distribution of concentrations sampled by olfactory organs at different locations on the body of an arthropod can provide important cues for plume tracking (reviewed by Derby and Steullet, 2001; Webster et al., 2001; Webster and Weissburg, 2009; Gomez-Marin et al., 2010). Both lobsters and crabs have olfactory sensors on their walking legs as well as their antennules, and although these animals can locate an odor source using only antennule or only leg sensors, they do so more quickly with both systems operating (Keller et al., 2003; Horner et al., 2004). For odor released from a source on the substratum, the variance in odor concentration is lower and the mean concentration is greater near the bed, where leg chemosensors continuously sample the plume, than higher in the water, where antennules sniff (Fig. 4). Therefore, it is not surprising that we found that the odor concentrations encountered by legs are more continuous than those intercepted by antennules (Figs 6 and 7 *vs* Fig. 15), as was observed for *C. sapidus* searching in a plume (Keller et al., 2003). Odor concentrations sampled by the legs increase as an animal nears an odor source (Fig. 15), whereas they decrease for antennules (Fig. 8); thus, leg olfactory sensors should become more important in locating the source when an animal is very near to it. We found striking differences in the concentrations encountered by leg sensors at the edge *vs* the centerline of a plume (Fig. 15), and

behavioral studies have shown that asymmetry of odor concentrations sampled by the right and left legs affects the movements of crabs transverse to an odor plume (Jackson et al., 2007; Dickman et al., 2009; Page et al., 2011b).

PLIF studies like ours that compare instantaneous odor sampling by olfactory organs with different designs and kinematics, coupled with PLIF studies of animal behaviors in response to encountered odors (Mead et al., 2003; Jackson et al., 2007; Dickman et al., 2009; Page et al., 2011a; Page et al., 2011b) can not only shed light on the cues animals use to find the sources of odors in turbulent natural habitats and provide templates for realistic patterns of odor delivery for use in neurobiological experiments but also provide insights for the design of chemical sensors and odor-tracking algorithms for man-made vehicles.

LIST OF SYMBOLS AND ABBREVIATIONS

c	instantaneous concentration
$\bar{c}$	mean concentration
c_{source}	source concentration
C_d	coefficient of drag
D	molecular diffusivity
D_{aesth}	diameter of aesthetasc hair
H	water depth in flume
L	length of flume from beginning of test section
P	probability
PIV	particle image velocimetry
PLIF	planar laser induced fluorescence
Re	Reynolds number
Re^*	roughness Reynolds number
Sc	Schmidt number
t	time
u	mean velocity of the fluid, measured at z=0.1 m
$u(z)$	mean velocity of fluid at height z
u^*	friction velocity
u_{flick}	velocity of antennule flick
x	downstream distance from plume source
y	transverse distance from plume centerline
z	vertical distance from flume bed
z_o	roughness length scale
δ	turbulent boundary layer thickness
κ	von Karman's constant
ν	kinematic viscosity of the fluid
σ	standard deviation

ACKNOWLEDGEMENTS

We thank Nicole George and Rudi Schuech for help with data collection and John Porter for help with statistical analysis. This research was supported by a National Science Foundation grant CBET-0933034 and a Miller Institute Fellowship at U. C. Berkeley to M.A.R., and The Virginia G. and Robert E. Gill Chair to M.A.R.K.

REFERENCES

Ache, B. W. (1982). Chemoreception and thermoreception. In *The Biology of Crustacea, Vol. 3: Neurobiology: Structure and Function* (ed. H. L. Atwood and D. C. Sandeman), pp. 369-398. New York: Academic Press.

Ache, B. W. (1991). Phylogeny of taste and smell. In *Smell and Taste in Health and Disease* (ed. T. V. Getchell, R. L. Doty, L. M. Bartoshuk and J. B. Snow), pp. 3-18. Raven Press: New York.

Ache, B. W. and Derby, C. D. (1985). Functional organization of olfaction in crustaceans. *Trends Neurosci.* **8**, 356-360.

Ache, B. W. and Young, J. M. (2005). Olfaction: diverse species, conserved principles. *Neuron* **48**, 417-430.

Atema, J. (1998). Tracking turbulence: processing the bimodal signals that define an odor plume. *Biol. Bull.* **195**, 179-180.

Bau, J., Justus, K. A. and Carde, R. T. (2002). Antennal resolution of pulsed pheromone plumes in three moth species. *J. Insect Physiol.* **48**, 433-442.

Bau, J., Justus, K. A., Loudon, C. and Carde, R. T. (2005). Electroantennographic resolution of pulsed pheromone plumes in two species of moths with bipectinate antennae. *Chem. Senses* **30**, 771-780.

Borroni, P. F. and Atema, J. (1988). Adaptation in chemoreceptor cells I. Self-adapating backgrounds determine threshold and cause parallel shift of response function. *J. Comp. Physiol., A* **164**, 67-74.

Bossert, W. H. and Wilson E. O. (1963). Analysis of olfactory communication among animals. *J. Theor. Biol.* **5,** 443-469.

Cardé, R. T. and Willis, M. A. (2008). Navigational strategies used by insects to find distant, wind-borne sources of odor. *J. Chem. Ecol.* **34**, 854-866.

Corotto, F. S. and Michel, W. C. (1998). Mechanisms of afterhyperpolarization in lobster olfactory receptor neurons. *J. Neurophysiol.* **80**, 1268-1276.

Crimaldi, J. P. (2008). Planar laser induced fluorescence in aqueous flows. *Exper. Fluids* **44**, 851-863.

Crimaldi, J. P., Koehl, M. A. R. and Koseff, J. R. (2002a). Effects of the resolution and kinematics of olfactory appendages on the interception of chemical signals in a turbulent odor plume. *Environ. Fluid Mech.* **2**, 35-63.

Crimaldi, J. P., Wiley, M. B. and Koseff, J. R. (2002b). The relationship between mean and instantaneous structure in turbulent passive scalar plumes. *J. Turb.* **3**, 1-24.

Derby, C. D. and Steullet, P. (2001). Why do animals have so many receptors? The role of multiple chemosensors in animal perception. *Biol. Bull.* **200**, 211-215.

Derby, C. D., Steullet, P., Horner, A. J. and Cate, H. S. (2001). The sensory basis of feeding behaviour in the Caribbean spiny lobster, *Panulirus argus*. *Mar. Freshw. Res.* **52**, 1339-1350.

Devine, D. V. and Atema, J. (1982). Function of chemoreceptor organs in spatial orientation of the lobster, *Homarus americanus*: differences and overlap. *Biol. Bull.* **163**, 144-153.

Dickman, B. D., Webster, D. R., Page, J. L. and Weissburg, M. J. (2009). Three-dimensional odorant concentration measurements around actively tracking blue crabs. *Limnol. Oceanogr. Methods* **7**, 96-108.

Finelli, C. M., Pentcheff, N. D., Zimmer-Faust, R. K. and Wethey, D. S. (1999). Odor transport in turbulent flows: constraints on animal navigation. *Limnol. Oceanogr.* **44**, 1056-1071.

Garm, A., Shabani, S., Hoeg, J. T. and Derby, C. D. (2005). Chemosensory neurons in the mouthparts of the spiny lobsters *Panulirus argus* and *Panulirus interruptus* (Crustacea: Decapoda). *J. Exp. Mar. Biol. Ecol.* **314**, 175-186.

Gleeson, R. A. (1982). Morphological and behavioral identification of the sensory structures mediating pheromone reception in the blue crab, *Callinectes sapidus*. *Biol. Bull.* **163**, 162-171.

Gleeson, R. A., Carr, W. E. S. and Trapido-Rosenthal, H. G. (1993). Morphological characteristics facilitating stimulus access and removal in the olfactory organ of the spiny lobster, *Panulirus argus*: insight from the design. *Chem. Senses* **18**, 67-75.

Goldman, J. A. and Koehl, M. A. R. (2001). Fluid dynamic design of lobster olfactory organs: high speed kinematic analysis of antennule flicking by *Panulirus argus*. *Chem. Senses* **26**, 385-398.

Gomez, G. and Atema, J. (1996a). Temporal resolution in olfaction: stimulus integration time of lobster chemoreceptor cells. *J. Exp. Biol.* **199**, 1771-1779.

Gomez, G. and Atema, J. (1996b). Temporal resolution in olfaction ii: time course of recovery from adaptation in lobster chemoreceptor cells. *J. Neurophysiol.* **76**, 1340-1343.

Gomez, G., Voigt, R. and Atema, J. (1994). Frequency filter properties of lobster chemoreceptor cells determined with high-resolution stimulus measurement. *J. Comp. Physiol., A* **174**, 803-811.

Gomez, G., Voigt, R. and Atema, J. (1999). Temporal resolution in olfaction III: flicker fusion and concentration-dependent synchronization with stimulus pulse trains of antennular chemoreceptor cells in the American lobster. *J. Comp. Physiol., A* **185**, 427-436.

Gomez-Marin, A., Duistermars, B. J., Frye, M. A. and Louis, M. (2010). Mechanisms of odor-tracking: multiple sensors for enhanced perception and behavior. *Front. Cell. Neurosci.* **4**, 1-15.

Grasso, F. W. (2001). Invertebrate-inspired sensory-motor systems and autonomous, olfactory-guided exploration. *Biol. Bull.* **200**, 160-168.

Grasso, F. W. and Basil, J. A. (2002). How lobsters, crayfishes, and crabs locate sources of odor: current perspectives and future directions. *Curr. Opin. Neurobiol.* **12**, 721-727.

Gross, T. F. and Nowell, A. R. (1983). Mean flow and turbulence scaling in a tidal boundary layer. *Cont. Shelf Res.* **2**, 109-126.

Grunert, U. and Ache, B. W. (1988). Ultrastructure of the aesthetasc (olfactory) sensilla of the spiny lobster *Panulirus argus*. *Cell Tiss. Res.* **251**, 95-103.

Hays, W. L. (1994). *Statistics*. Fort Worth, TX: Wadsworth Publishing.

Hildebrand, J. G., and Shepherd, G. M. (1997). Mechanisms of olfactory discrimination: converging evidence for common principles across phyla. *Ann. Rev. Neurosci.* **20**, 595-631.

Horner, A. J., Weissburg, M. J. and Derby, C. D. (2004). Dual antennular chemosensory pathways can mediate orientation by Caribbean spiny lobsters in naturalistic flow conditions. *J. Exp. Biol.* **207**, 3785-3796.

Horner, A., Weissburg, M. J. and Derby, C. D. (2007). The olfactory pathway mediates sheltering behavior of Caribbean spiny lobsters, *Panulirus argus*, to conspecific urine signals. *J. Comp. Physiol., A* **194**, 243-253.

Jackson, J. L., Webster, D. R., Rahman, S. and Weissburg, M. J. (2007). Bed-roughness effects on boundary-layer turbulence and consequences for odor-tracking behavior of blue crabs (*Callinectes sapidus*). *Limnol. Oceanogr.* **52**, 1883-1897.

Junek, S., Kludt, E., Wolf, F. and Schild, D. (2010). Olfactory coding with patterns of response latencies. *Neuron* **67**, 872-884.

Justus, K. A. and Carde, R. T. (2002). Flight behaviour of males of two moths, *Cadra cautella* and *Pectinophora gossypiella*, in homogeneous clouds of pheromone. *Physiol. Entomol.* **27**, 67-75.

Justus, K. A., Murlis, J., Jones, C. and Cardé, R. T. (2002a). Measurement of odor-plume structure in a wind tunnel using a photoionization detector and a tracer gas. *Environ. Fluid Mech.* **2**, 115-142.

Justus, K. A., Schofield, S. W., Murlis, J. and Cardé, R. T. (2002b). Flight behaviour of *Cadra cautella* males in rapidly pulsed pheromone plumes. *Physiol. Entomol.* **27**, 58-66.

Justus, K. A., Cardé, R. T. and French, A. S. (2005). Dynamic properties of antennal responses to pheromone in two moth species. *J. Neurophysiol.* **93**, 2233-2239.

Keller, T. A. and Weissburg, M. J. (2004). Effects of odor flux and pulse rate on chemosensory tracking in turbulent odor plumes by the blue crab, *Callinectes sapidus*. *Biol. Bull.* **207**, 44-55.
Keller, T. A., Powell, I. and Weissburg, M. J. (2003). Role of olfactory appendages in chemically mediated orientation of blue crabs. *Mar. Ecol. Progr. Ser.* **261**, 217-231.
Koehl, M. A. R. (2001). Fluid dynamics of animal appendages that capture molecules: arthropod olfactory antennae. In *Computational Modeling in Biological Fluid Dynamics*, (ed. L. J. Fauci and S. Gueron). New York: Springer.
Koehl, M. A. R. (2006). The fluid mechanics of arthropod sniffing in turbulent odor plumes. *Chem. Senses* **31**, 93-105.
Koehl, M. A. R. (2011). Hydrodynamics of sniffing by crustaceans. In *Chemical Communication in Crustaceans* (ed. T. Breithaupt and M. Theil), pp. 85-102. New York: Springer Verlag.
Koehl, M. A. R., Koseff, J. R., Crimaldi, J. P., McCay, M. G., Cooper, T., Wiley, M. B. and Moore, P. A. (2001). Lobster sniffing: Antennule design and hydrodynamic filtering of information in an odor plume. *Science* **294**, 1948-1951.
Krofczik, S., Menzel, R. and Nawrot, M. P. (2008). Rapid odor processing in the honeybee antennal lobe network. *Front. Comput. Neurosci.* **2**, 1-13.
Laurent, G., Stopfer, M., Friedrich, R. W., Rabinovich, M. I., Volkovskii, A. and Abarbanel, H. D. I. (2001). Odor encoding as an active, dynamical process: experiments, computation, and theory. *Ann. Rev. Neurosci.* **24**, 263-297
Lei, H., Riffell, J. A., Gage, S. L. and Hildebrand, J. G. (2009). Contrast enhancement of stimulus intermittency in a primary olfactory network and its behavioral significance. *J. Biol.* **8**, 21.1-21.15.
Lo Iacono, G. and Reynolds, A. M. (2008). Modelling of concentrations along a moving observer in an inhomogeneous plume. Biological application: model of odour-mediated insect flights. *Environ. Fluid Mech.* **8**, 147-168.
Mafra-Neto, A. and Cardé, R. T. (1995). Effect of the fine-scale structure of pheromone plumes-pulse frequency modulates activation and upwind flight of almond moth males. *Physiol. Entomol.* **20**, 229-242.
Mafra-Neto, A. and Cardé, R. T. (1996). Dissection of the pheromone-modulated flight of moths using single-pulse response as a template. *Experientia* **52**, 373-379.
Mafra-Neto, A. and Cardé, R. T. (1998). Rate of realized interception of pheromone pulses in different wind speeds modulates almond moth orientation. *J. Compar. Physiol. A* **182**, 563-572.
Marschall H. P. and Ache, B. W. (1989). Response dynamics of lobster olfactory neurons during simulated natural sampling. *Chem. Senses* **14**, 725.
Mead, K. S. (2002). From odor molecules to plume tracing: an interdisciplinary, multilevel approach to olfaction in stomatopods. *Integr. Comp. Biol.* **42**, 258-264.
Mead, K. S. and Koehl, M. A. R. (2000). Stomatopod antennule design: the asymmetry, sampling efficiency, and ontogeny of olfactory flicking. *J. Exp. Biol.* **203**, 3795-3808.
Mead, K. S., Wiley, M. B., Koehl, M. A. R. and Koseff, J. R. (2003). Fine-scale patterns of odor encounter by the antennules of mantis shrimp tracking turbulent plumes in wave-affected and unidirectional flow. *J. Exp. Biol.* **206**, 181-193.
Mellon, D. (2007). Combining dissimilar senses: Central processing of hydrodynamic and chemosensory inputs in aquatic crustaceans. *Biol. Bull.* **213**, 1-11.
Monteclaro, H. M., Anraku, K. and Matsuoka, T. (2010). Response properties of crayfish antennules to hydrodynamic stimuli: functional differences in the lateral and medial flagella. *J. Exp. Biol.* **213**, 3683-3691.
Moore, P. A. and Atema, J. (1991). Spatial Information in the 3-dimensional fine scale structure of an aquatic odor plume. *Biol. Bull.* **181**, 408-418.
Moore, P. and Crimaldi, J. P. (2004). Odor landscapes and animal behavior: tracking odor plumes in different physical worlds. *J. Mar. Sys.* **49**, 55-64.
Murlis, J., Willis, M. A. and Carde, R. T. (2000). Spatial and temporal structures of pheromone plumes in fields and forests. *Physiol. Entomol.* **25**, 211-222.
Page, J. L., Dickman, B. D., Webster, D. R. and Weissburg, M. J. (2011a). Getting ahead: context-dependent responses to odorant filaments drive along-stream progress during odor tracking in blue crabs. *J. Exp. Biol.* **214**, 1498-1512.
Page, J. L., Weissburg, M. J., Dickman, D. B. and Webster, D. R. (2011b). Staying the course: the role of chemical signal spatial properties in navigation through turbulent plumes. *J. Exp. Biol.* **214**, 1513-1522.
Reidenbach, M. A., George, N. T. and Koehl, M. A. R. (2008). Antennule morphology and flicking kinematics facilitate odor sampling by the spiny lobster, *Panulirus argus*. *J. Exp. Biol.* **211**, 2849-2858.
Riffell, J. A., Abrell, L. and Hildebrand, J. G. (2008). Physical processes and real-time chemical measurement of the insect olfactory environment. *J. Chem. Ecol.* **34**, 837-853.
Rumbo, E. R. and Kaissling, K. E. (1989). Temporal resolution of odour pulses by three types of pheromone receptor cells in *Antheraea polyphemus*. *J. Comp. Physiol., A* **165**, 281-291.
Schlichting, H. and Gersten, K. (2000). *Boundary Layer Theory*. New York: Springer-Verlag.
Schmitt, B. C. and Ache, B. W. (1979). Olfaction: responses of a decapod crustacean are enhanced by flicking. *Science* **205**, 204-206.
Schoenfeld, T. A. (2006). Introduction to special issue: what's in a sniff? *Chem. Senses* **31**, 91-92.
Stacey, M. T., Mead, K. S. and Koehl, M. A. R. (2002). Molecule capture by olfactory antennules: Mantis shrimp. *J. Math. Biol.* **44**, 1-30.
Stengl, M. (2010). Pheromone transduction in moths. *Front. Cell. Neurosci.* **4**, 1-15.
Steullet, P., Krutzfeldt, D. R., Hamidani, G., Flavus, T., Ngo, V. and Derby, C. D. (2002). Dual antennular chemosensory pathways mediate odor-associative learning and odor discrimination in the Caribbean spiny lobster *Panulirus argus*. *J. Exp. Biol.* **205**, 851-867.
Su, C. Y., Menuz, K. and Carlson, J. R. (2009). Olfactory perception: receptors, cells, and circuits. *Cell* **139**, 45-59.
Tripathy, S. J., Peters, O. J., Staudacher, E. M., Kalwar, F. R., Hatfield, M. N. and Daly, K. C. (2010). Odors pulsed at wing beat frequencies are tracked by primary olfactory networks and enhance odor detection. *Front. Cell. Neurosci.* **4**, 1-14.
Vetter, R. S., Sage, A. E., Justus, K. A., Carde, R. T. and Galizia, C. G. (2006). Temporal integrity of an airborne odor stimulus is greatly affected by physical aspects of the odor delivery system. *Chem. Senses* **31**, 359-369.
Vickers, N. J. (2006). Winging it: moth flight behavior and responses of olfactory neurons are shaped by pheromone plume dynamics. *Chem. Senses* **31**, 155-166.
Vickers, N. J. and Baker, T. C. (1994). Reiterative responses to single strands of odor promote sustained upwind flight and odor source location by moths. *Proc. Natl. Acad. Sci. USA* **91**, 5756-5760.
Vickers, N. J. and Baker, T. C. (1996). Latencies of behavioral response to interception of filaments of sex pheromone and clean air influence flight track shape in *Heliothis virescens* (F.) males. *J. Comp. Physiol. A* **178**, 831-847.
Vickers, N. J., Christensen, T. A., Baker, T. C. and Hildebrand, J. G. (2001). Odour-plume dynamics influence the brain's olfactory code. *Nature* **410**, 466-470.
Webster, D. R. and Weissburg, M. J. (2001). Chemosensory guidance cues in a turbulent chemical odor plume. *Limnol. Oceanogr.* **46**, 1034-1047.
Webster, D. R. and Weissburg, M. J. (2009). The hydrodynamics of chemical cues among aquatic organisms. *Ann. Rev. Fluid Mech.* **41**, 73-90.
Webster, D. R., Rahman, S. and Dasi, L. P. (2001). On the usefulness of bilateral comparison to tracking turbulent chemical odor plumes. *Limnol. Oceanogr.* **46**, 1048-1053.
Weissburg, M. J. and Zimmer-Faust, R. K. (1993). Life and death in moving fluids: hydrodynamic effects on chemosensory-mediated predation. *Ecology* **74**, 1428-1443.
Weissburg, M. J. and Zimmer-Faust, R. K. (1994). Odor plumes and how blue crabs use them to find prey. *J. Exp. Biol.* **197**, 349-375.
Willis, M. A. and Avondet, J. L. (2005). Odor-modulated orientation in walking male cockroaches *Periplaneta americana*, and the effects of odor plumes of different structure. *J. Exp. Biol.* **208**, 721-735.
Willis, M. and Baker, T. C. (1984). Effects of intermittent and continuous pheromone stimulation on the flight behaviour of the oriental fruit moth *Grapholita molesta*. *Physiol. Entomol.* **9**, 341-354.
Wilson, R. I. (2008). Neural and behavioral mechanisms of olfactory perception. *Curr. Opin. Neurobiol.* **18**, 408-412.
Wolf, M. C., Voigt, R. and Moore, P. A. (2004). Spatial arrangement of odor sources modifies the temporal aspects of crayfish search strategies. *J. Chem. Ecol.* **30**, 501-517.
Zettler, E. and Atema, J. (1999). Chemoreceptor cells as concentration slope detectors: Preliminary evidence from the lobster nose. *Biol. Bull.* **197**, 252-253.